







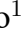






Original Research

Clinical, Immunological, and Vesicular Markers in Sarcopenia and Presarcopenia

Liudmila M. Shuliko¹, Dmitry A. Svarovsky^{1,2}, Liudmila V. Spirina^{1,2,*},
Ikponmwosa Jude Ogieuhi¹, Olga E. Akbasheva¹, Mariia V. Matveeva¹,
Iuliia G. Samoiloova^{1,3}, Valeria A. Shokalo¹, Sofia S. Timoshenko¹,
Sofia M. Merkulova¹, Amin I. Ragimov¹, Mar'yam P. Shukyurova¹,
Natalia V. Tarasenko¹

¹Division of Biochemistry and Molecular Biology, Siberian State Medical University, Ministry of Health of the Russian Federation, 634050 Tomsk, Russia

²Cancer Research Institute, Tomsk National Research Medical Center, 634050 Tomsk, Russia

³Institute of Medicine and Medical Technologies, Federal State Autonomous Educational Institution of Higher Education, National Research State University, 630090 Novosibirsk, Russia

*Correspondence: spirinalvl@mail.ru (Liudmila V. Spirina)

Academic Editors: Wei-Lin Jin and Amedeo Amedei

Submitted: 21 May 2025 Revised: 21 July 2025 Accepted: 25 July 2025 Published: 27 August 2025

Abstract

Background: Sarcopenia is a complex, multifactorial condition characterized by progressive loss of muscle mass, strength, and function. Despite growing awareness, the early diagnosis and pathophysiological characterization of this condition remain challenging due to the lack of integrative biomarkers. **Objective:** This study aimed to conduct a comprehensive multilevel profiling of clinical parameters, immune cell phenotypes, extracellular vesicle (EV) signatures, and biochemical markers to elucidate biological gradients associated with different stages of sarcopenia. **Materials and Methods:** A prospective cohort study enrolled adults aged 45–85 years classified as control, presarcopenic, or sarcopenic based on European Working Group on Sarcopenia in Older People 2 (EWGSOP2) criteria. Clinical evaluation included anthropometry, muscle strength, sarcopenia screening (SARC-F) questionnaire/Short Physical Performance Battery (SPPB) questionnaires, and quality-of-life assessment. Flow cytometry was used to characterize blood monocyte/macrophage subsets (cluster of differentiation 14 (CD14), CD68, CD163, CD206). EVs were isolated from plasma and profiled for surface tetraspanins and matrix metalloproteinases (MMP2, MMP9, tissue inhibitor of metalloproteinase-1 (TIMP-1)) using bead-based flow cytometry. Biochemical assays measured metabolic, inflammatory, and extracellular matrix (ECM)-related markers. Data were analyzed via Kruskal–Wallis testing, discriminant analysis, and principal component analysis (PCA). **Results:** Sarcopenia, a muscle-wasting condition linked to aging, is characterized by chronic inflammation, proteolytic imbalance, and metabolic disturbances. Clinical deterioration is evident through reduced appendicular lean mass (ALM), appendicular skeletal muscle index (ASMI), SPPB scores, and sarcopenia quality of life (SarQoL) domains. Principal component analysis (PCA) identified four functional marker clusters: ECM degradation (MMP-positive EVs), inflammatory and homeostasis-stabilizing macrophages, and metabolic disruption (glucose, asprosin, triglycerides). Discriminant analysis emphasized vesicular and immune markers with significant classification potential, even when univariate differences were non-significant. Metabolic destabilization and inflammatory activation are detectable in presarcopenia stages. Chronic inflammation, characterized by CD14–CD163+206+ cells releasing pro-inflammatory cytokines, accelerates muscle degradation. Proteolytic dysfunction, with an imbalance between proteases and inhibitors, further contributes to muscle loss. Metabolic disorders impair energy production and nutrient utilization, exacerbating muscle wasting. A comprehensive assessment, including anthropometric, functional, physical activity, and QoL measures, is crucial for identifying high-risk individuals and understanding sarcopenia's mechanisms. Vesicular biomarkers, regulating tissue remodeling and inflammation, provide valuable insights. Standardized assessment methods are essential for enhancing diagnostic accuracy and intervention effectiveness. Future research should focus on developing and refining biomarkers to improve specificity and sensitivity, enabling targeted therapies and better QoL. **Conclusions:** Integrating clinical, immunological, and biochemical markers with EVs helps stratify sarcopenia effectively. Our data shows that EVs and macrophage profiles reflect systemic changes and metabolic stress. However, age- and gender-related variability in our cohort warrants caution in generalizing the findings. Artificial intelligence (AI) enhances patient clustering by combining these data types, enabling precise, personalized sarcopenia management, predicting disease progression, and identifying high-risk patients. AI also standardizes and optimizes analytical protocols, improving diagnostic and monitoring reliability and reproducibility.

Keywords: sarcopenia; monocytes; macrophages; extracellular vesicles; matrix metalloproteinases; vitronectin; proteases; α 1-antitrypsin; asprosin; meteorin-like protein



1. Introduction

Sarcopenia, a progressive muscle disorder characterized by reduced strength, quality, and quantity leading to impaired mobility and poor quality of life, is a significant public health issue due to its association with morbidity, mortality, and increased healthcare costs [1,2]. As global populations age, its prevalence rises, often coexisting with osteoporosis and frailty.

The condition's pathophysiology involves complex biochemical markers such as myokines, growth factors, microRNAs, and metabolic regulators, though their clinical application is still debated [3]. Standard care guidelines emphasize low muscle strength as the primary indicator, with screening tools like the sarcopenia screening questionnaire (SARC-F) questionnaire and Dual-energy X-ray Absorptiometry (DXA) scans recommended [4]. Regional variations exist, with notable differences in the Asian Working Group for Sarcopenia (AWGS) and European Working Group on Sarcopenia in Older People 2 (EWGSOP2) guidelines [5].

Sarcopenia is multifactorial, influenced by genetics, environment, and lifestyle. Risk factors include sociodemographic characteristics, health behaviors, health conditions, biomarkers, early life experiences, and living environments [1]. A study in Pakistan found a high prevalence of 47.18%, with higher rates in males and a strong correlation with age [2]. Sarcopenia affects 5%–13% of community-dwelling older adults aged 60+, rising to nearly 50% among those over 80 [3]. It increases the risk of falls, fractures, hospitalization, cognitive impairment, and mortality, making early diagnosis and intervention crucial.

Anti-inflammatory macrophages are typical for the control group [6], while the activation of inflammatory macrophages increases with sarcopenia [7]. The spleen, as the main immune organ, is particularly involved in chronic low-grade inflammation [8]. Sarcopenia, on the other hand, is central to systemic inflammation in aging [9]. Liver disease, particularly nonalcoholic fatty liver disease (NAFLD), characterized by systemic inflammation, is also associated with sarcopenia, as revealed data indicate [10].

Empirical evidence robustly supports a correlation between the spleen and liver, aligning with the established concept of the liver-spleen axis in NAFLD [11]. This interorgan communication network has been extensively investigated in NAFLD pathogenesis, highlighting the pivotal role of metabolic crosstalk between hepatic and splenic tissues [11].

Active extracellular matrix (ECM) degradation is a key feature of sarcopenia [12], and metalloproteinase inhibitors are involved in the imbalance observed in sarcopenia [13]. Connective tissue destruction is activated in sarcopenia, which is further supported by studies [14–18].

The complex ECM remodeling imbalance is characterized by ECM destruction without inhibitory control.

In the presarcopenic stage, controlled matrix metalloproteinase (MMP) activation is typical, indicating a balanced ECM degradation during the transitional phase [19,20]. Enhanced ECM destruction is observed in sarcopenia, and active ECM destruction is prominent in late-stage sarcopenia [20]. Vitronectin, which modulates cell adhesion, is decreased in sarcopenia [21,22], contributing to the impaired tissue integrity.

Sarcopenia is associated with dysregulation of glucose metabolism [23]. Myokine response to inflammation may serve as a compensatory mechanism [24], while glucose metabolism disturbances are closely linked to sarcopenia [25,26]. Dyslipidemia is a metabolic component of sarcopenia, contributing to muscle dysfunction [27].

Insulin secretion is impaired in sarcopenia, indicating insulin resistance [28]. Destruction of elastic fibers and tissue remodeling are also observed in sarcopenia [29], further compromising tissue integrity. Total protein levels, reflecting general nutritional status, are decreased in sarcopenia [30,31], highlighting the role of malnutrition in sarcopenia development. Acute phase inflammation is activated in sarcopenia, contributing to the inflammatory milieu [32] and exacerbating muscle wasting. The imbalance of proteolysis is a crucial pathogenic process, which can be related to the activity of proteolytic enzymes such as trypsin-like and elastase-like proteinases. These enzymes play a significant role in tissue remodelling and inflammation. The equilibrium between their activity and that of inhibitors, such as α 1-antitrypsin, is essential for maintaining tissue homeostasis. Dysregulation of this balance can lead to various pathological conditions. This study aimed to conduct a comprehensive multilevel profiling of clinical parameters, immune cell phenotypes, extracellular vesicle (EV) signatures, and biochemical markers to elucidate biological gradients associated with different stages of sarcopenia.

2. Materials and Methods

From September 2024 to March 2025, a pilot prospective uncontrolled cohort single-center study was conducted in parallel groups within the framework of the project “Biochemical and Pathogenetic Features of Chronic Non-Communicable Disease Development” affiliated with the Siberian State Medical University.

The study was approved by the Ethics Committee of the Siberian State Medical University (protocol No. 10000, dated January 20, 2024).

2.1 Inclusion and Exclusion Criteria of the Study

2.1.1 Inclusion Criteria

Individuals aged 45 to 85 years were eligible for participation upon signing an informed consent form covering all procedures outlined in the study protocol.

2.1.2 Exclusion Criteria

Participants were excluded if they presented with one or more of the following conditions or factors: acute or chronic diseases in the decompensation stage (including cardiovascular, respiratory, gastrointestinal, urinary, or other systems); severe musculoskeletal disorders; presence of electronic cardiac rhythm-regulating devices; any conditions in which physical performance testing might pose a risk to the participant's health or life; pregnancy.

2.1.3 Clinical Assessment

Medical history and physical examination were performed to confirm eligibility based on inclusion and exclusion criteria and to identify sarcopenia risk factors. These included medication histories, living conditions, harmful habits, presence of chronic diseases, previous trauma, prolonged immobilization, or surgical interventions requiring extended hospitalization.

2.1.4 Anthropometric Measurements

Body weight was measured to the nearest 0.1 kg using the built-in scale of the InBody 770 body composition analyzer (InBody Co., Seoul, South Korea). Measurements were taken in the morning, in underwear, with an empty bladder and on an empty stomach. Height was measured to the nearest 0.1 cm using the MSK-233 stadiometer (MSK-233, Moscow, Moscow region, Russia), without shoes. Waist and hip circumferences were measured with a tape measure, accurate to 10 mm. The results were used to calculate body mass index (BMI) as weight (kg) / height² (m²) and waist-to-hip ratio.

2.1.5 Muscle Strength Assessment

Handgrip strength was assessed using a DK-140 hand dynamometer (JSC "Nizhny Tagil Medical Instrument Plant", Nizhny Tagil, Russia). Participants performed three measurements with their dominant hand, and the final result was calculated as the arithmetic mean of the three attempts. All measurements were conducted in a seated position, with the shoulder adducted and neutrally rotated, elbow flexed at 90°, forearm in a neutral position, and wrist between 0° and 30° dorsiflexion, following recommendations from the American Society of Hand Therapists. The device was zeroed prior to each measurement session. Reduced grip strength was defined as <27 kg for men and <16 kg for women.

2.1.6 Assessment of Muscle Mass

Muscle mass was measured using the InBody 770 analyzer (InBody Co., Seoul, South Korea) utilizing 8-point tactile tetrapolar multi-frequency bioelectrical impedance analysis. The device was calibrated according to manufacturer recommendations before each measurement session. Participants were instructed to refrain from physical activity, caffeine, and food intake for at least 2 hours

prior to assessment. All measurements were performed in the morning, under standardized conditions. Appendicular lean mass (ALM) was recorded, and appendicular skeletal muscle index (ASMI) was calculated as ALM (kg) divided by height squared (m²). Low muscle mass was defined as ASMI <7.0 kg/m² for men and <5.5 kg/m² for women.

2.1.7 Functional Muscle Performance

Functional performance was assessed using the SPPB. The 4-meter gait speed test was conducted on a flat, unobstructed surface, with participants starting from a static standing position. Timing started when the participant-initiated movement and stopped when one foot completely crossed the 4-meter mark. A trained evaluator provided verbal encouragement and ensured consistent measurement technique. An SPPB score of ≤8 points indicated reduced muscle function. The battery included a 4-meter gait speed test, where a result of ≤0.8 m/s was considered diagnostic for sarcopenia.

2.1.8 Sarcopenia Screening and Quality of Life Evaluation

Sarcopenia screening was conducted using the SARC-F questionnaire, which includes five questions assessing signs of reduced muscle strength: difficulty in lifting weights, walking, standing up from a chair, climbing stairs, and falling [1]. Each question offered three response options. A total score of more than 4 was interpreted as probable sarcopenia. Quality of life was assessed using the sarcopenia quality of life (SarQoL) questionnaire, consisting of 22 questions grouped into seven domains: D1 "Physical and Mental Health"; D2 "Mobility"; D3 "Body Composition"; D4 "Functionality"; D5 "Activities of Daily Living"; D6 "Leisure"; and D7 "Fears". Each domain was scored from 0 to 100, with higher scores indicating better quality of life. This evaluation was supplemented by the SF-36 questionnaire, assessing physical (SF-36 PH) and mental (SF-36 MH) well-being on a scale from 0 to 100, where higher scores reflect better quality of life in the respective domains. Physical activity levels were assessed using the international physical activity questionnaire (IPAQ) [2]; physical inactivity was verified at <14 points for individuals under 65 years and <7 points for those over 65 years.

2.1.9 Study Cohort

A total of 55 participants were included in the study, stratified into control (n = 25), presarcopenia (n = 18), and sarcopenia (n = 12) groups. Gender distribution was unequal across groups, with some gender-specific subgroups comprising as few as 2 individuals. Participants were classified into three groups according to the EWGSOP2-2019 criteria based on the presence or absence of sarcopenia indicators [3]. All descriptive statistics are shown in Table 1.

Control group (25 participants: 18 men, 7 women): clinically healthy individuals without signs of reduced muscle strength, mass, or function. Presarcopenia group (18

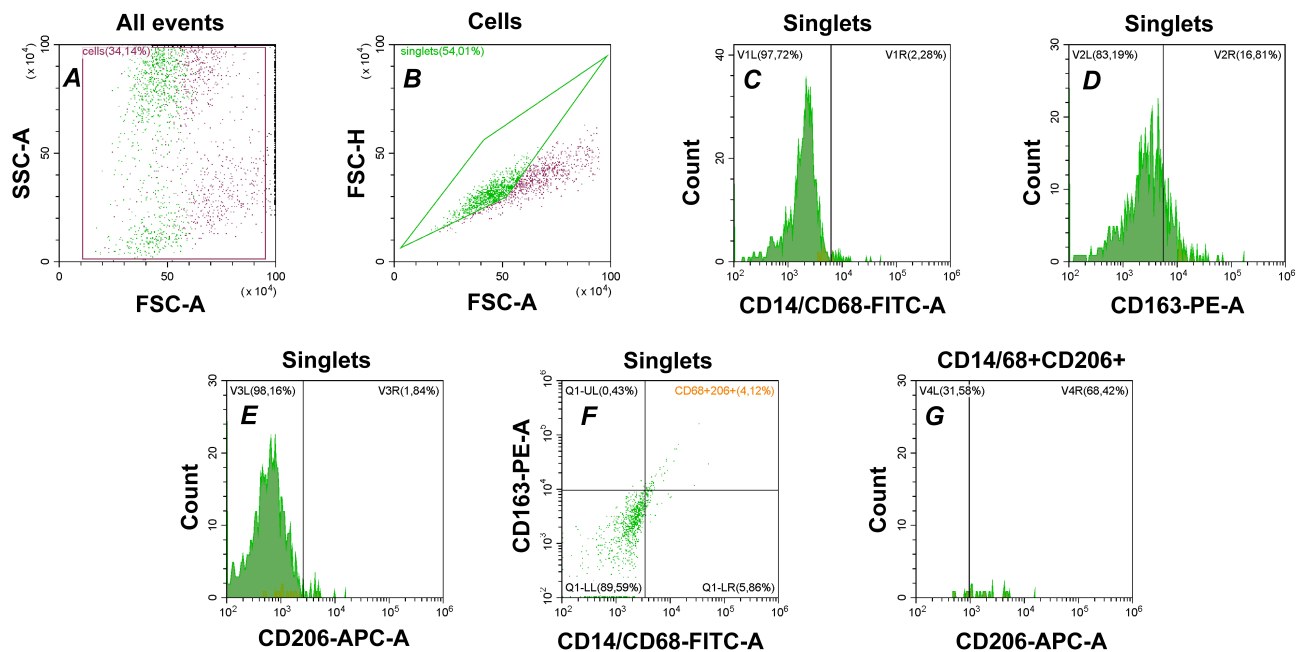


Fig. 1. Analysis of CD14- and CD68-positive cell subpopulations in blood samples. (A) Identification of target cells based on forward (FSC-A) and side scatter (SSC-A) light parameters with gating strategy applied. (B) Selection of singlet events from the total gated cell population. (C) Histogram showing the distribution of CD14+ or CD68+ cells among singlets in gate. (D) Detection of CD163+ cells within the singlet gate. (E) Detection of CD206+ cells within the singlet population. (F) Dual staining analysis of CD14 or CD68 together with CD163 among singlet events, with quadrant gates indicating the proportions of cell subsets based on CD14+/CD68+ and CD163 expression. (G) Histogram showing the distribution of CD206+ cells within the CD14+CD163+ or CD68+CD163+ cell populations. SSC-A, side scatter area; FSC-A, forward scatter area; APC-A, allophycocyanin; FITC-A, fluorescein isothiocyanate; PE-A, phycoerythrin; CD, cluster of differentiation.

Table 1. Description of the study cohort.

Group	Sex (Men = 1, Women = 2)	n (%)	<i>p</i>	Age, years (Mean ± SD)
Control	1	18 (32.7)	—	58.5 ± 8.625
	2	7 (12.7)	—	61.57 ± 8.149
Presarcopenia	1	14 (25.5)	0.12	68.43 ± 11.68
	2	4 (7.3)	0.34	64.5 ± 18.806
Sarcopenia	1	10 (18.2)	0.04	75.2 ± 8.149
	2	2 (3.6)	0.06	77.5 ± 2.121

SD, standard deviation.

participants: 14 men, 4 women): participants with isolated low muscle strength but preserved functional status and muscle mass. Sarcopenia group (12 participants: 10 men, 2 women): individuals meeting all three criteria—reduced muscle strength, decreased muscle mass, and impaired muscle function. The median age of sarcopenic patients (74.0 years) was significantly higher than that of controls (58.0 years), $p = 0.0001$.

2.2 Flow Cytometry Analysis of Mononuclear Cells

Patient whole blood aliquots (100 μ L) were incubated with the following antibodies for 20 minutes in the dark: FITC Anti-Human CD14 Antibody (1:100, AN00420C, Elabscience, Wuhan, Hubei, China), PE Anti-Human

CD163 Antibody (1:100, GHI/61, BioLegend, Shanghai, China), APC Anti-Human CD206/MMR Antibody (1:100, E-AB-F1161E, Elabscience, China), FITC Anti-Human CD68 Antibody (1:100, E-AB-22013, Elabscience, China). Following staining, erythrocytes were lysed using Erythrolyse Red Blood Cell Lysing Buffer (10 \times) (Bio-Rad, Berkeley, CA, USA) and samples were triple-washed in phosphate-buffered saline (PBS, PanEko, Russia) by centrifugation at 3000 g for 5 minutes. After washing, the samples were mixed manually and analyzed by a Cytoflex flow cytometer (Beckman Coulter, Brea, CA, USA) (Fig. 1). All cell lines were validated by STR profiling and tested negative for mycoplasma.

2.3 Extracellular Vesicles Isolation and Characterization

2.3.1 Isolation and Typing of EVs

Extracellular vesicles were obtained through a combination of ultrafiltration and ultracentrifugation techniques. Venous blood (27 mL) was drawn into K3EDTA-coated vacutainers. Initial cell separation was carried out by centrifugation at $1000 \times g$ for 20 minutes at 4°C . The plasma supernatant was carefully transferred to a new tube and subjected to a second centrifugation step at $14,000 \times g$ for 15 minutes at 4°C . The resulting supernatant was then diluted with PBS to a final volume of 33 mL and passed through a 220 nm pore-size filter (PES membrane, Wuxi NEST Biotechnology Co., Ltd., Wuxi, China).

The filtered plasma was subsequently ultracentrifuged using a bucket rotor (Optima XPN 80, Beckman Coulter, Brea, CA, USA) at 4°C for 90 minutes. The pellet obtained after ultracentrifugation was resuspended in PBS and centrifuged again under the same conditions to further purify the extracellular vesicles (EVs). The resulting EV aliquots were frozen in liquid nitrogen and stored at -80°C until further analysis.

The size distribution and concentration of isolated vesicles were evaluated by nanoparticle tracking analysis (NTA) on a NanoSight® LM10 system (Malvern Instruments, Worcestershire, UK). For optimal NTA measurements, the EV samples were diluted with PBS at ratios of 1:100, 1:1000, and 1:10,000. Each sample underwent a one-minute analysis to determine the mean vesicle size, size distribution profile, and particle concentration.

For transmission electron microscopy (TEM) imaging, the EVs were adsorbed onto copper grids pre-coated with a formvar-carbon film, followed by negative staining with 2% phosphotungstic acid. The prepared grids were then examined using a Talos L120C electron microscope (Thermo Fisher Scientific, Waltham, MA, USA).

2.3.2 Tetraspanin Profiling of EVs

4 μm aldehyde/sulfate latex beads (5 μL ; Molecular Probes, Eugene, OR, USA) were washed twice with 100 μL 0.1 M MES buffer (pH 5.5) by centrifugation ($3000 \times g$, 15 min, room temperature), resuspended in 25 μL MES, and incubated with 3 μg anti-CD9 antibodies (1:1500; SAA0003, Antibody System, France) for 14 h at room temperature with agitation. EV aliquots ($\sim 30 \mu\text{g}$ protein) were then incubated with 3×10^5 antibody-coated beads in 150 μL PBS at 4°C for 14 h. Binding was blocked using 0.2 M glycine for 30 min at 4°C . Complexes were washed twice with 2% EV-depleted bovine serum in PBS and treated with 5 μL Fc receptor binding inhibitor (14-9161-73; Invitrogen, CA, USA) for 10 min at room temperature.

For tetraspanin analysis, FITC-conjugated anti-CD63, anti-CD81, and anti-CD24 antibodies (1:100, 556019; 1:100, 555675; 1:100, 562439; BD Biosciences, Germany; 5 μL /test) were added to the complexes, followed by 20 min incubation and washing. Flow cytometry was conducted

using a CytoFLEX cytometer (Beckman Coulter, Brea, CA, USA) and data were analyzed with CytExpert 2.4. median fluorescence intensity (MFI) was compared against isotype and negative controls (BD Biosciences, USA). In immunofluorescence staining, negative controls are essential for verifying the accuracy and reliability of results. They distinguish specific from nonspecific staining.

Typing of EVs was performed in accordance with the recommendations of the International Society for Extracellular Vesicles (ISEV) [33]. The characterization data, including TEM, NTA and profiling of major tetraspanins, are presented in Fig. 2.

2.3.3 MMPs Profiling on CD9-Positive EVs

Complexes of CD9 antibody-coated aldehyde/sulfate latex beads with EVs were prepared as previously described. The resulting bead–EV complexes were washed twice with washing buffer and incubated with 5 μL of an anti-human Fc receptor binding inhibitor at room temperature for 10 minutes, followed by an additional wash.

For the detection of matrix metalloproteinases, the complexes were stained with FITC-conjugated anti-MMP9 (1:150; FAA553Hu81, Cloud-Clone Corp., Wuhan, China; 2 μL /test), PE-conjugated anti-MMP2 (1:150; FAA100Hu41, Cloud-Clone Corp., China; 2 μL /test), and APC-conjugated anti-tissue inhibitor of metalloproteinase-1 (TIMP-1) (1:150; FAA552Hu51, Cloud-Clone Corp., China; 2 μL /test) antibodies. Staining was performed for 20 minutes at room temperature, after which the samples were washed again.

Flow cytometric analysis was carried out using a CytoFLEX cytometer, and data were processed with CytExpert 2.0 software (Beckman Coulter, Brea, CA, USA). During acquisition, bead populations carrying EVs (“Beads” gate) were first identified, and 10,000 events per sample were collected at a high flow rate. The results of MMPs profiling are shown in Fig. 3.

2.4 Statistical Analysis

2.4.1 Kruskal–Wallis and Discriminant Analysis Results

Data analysis was conducted using specialized software packages: Statistica 12.0 (TIBCO, Palo Alto, CA, USA), JASP 0.19.3 (Eric-Jan Wagenmakers, Department of Psychological Methods, University of Amsterdam, Netherlands), and SPSS 28.0.1 (IBM, New York, NY, USA).

The normality of data distributions was assessed using the Shapiro–Wilk test and, where necessary, the Liliefors correction. Differences between multiple independent groups were analyzed using Kruskal–Wallis test and discriminant analysis, with statistical significance set at $p < 0.05$. The results of descriptive statistics were presented as the median and interquartile range (Me; (Q1; Q3)).

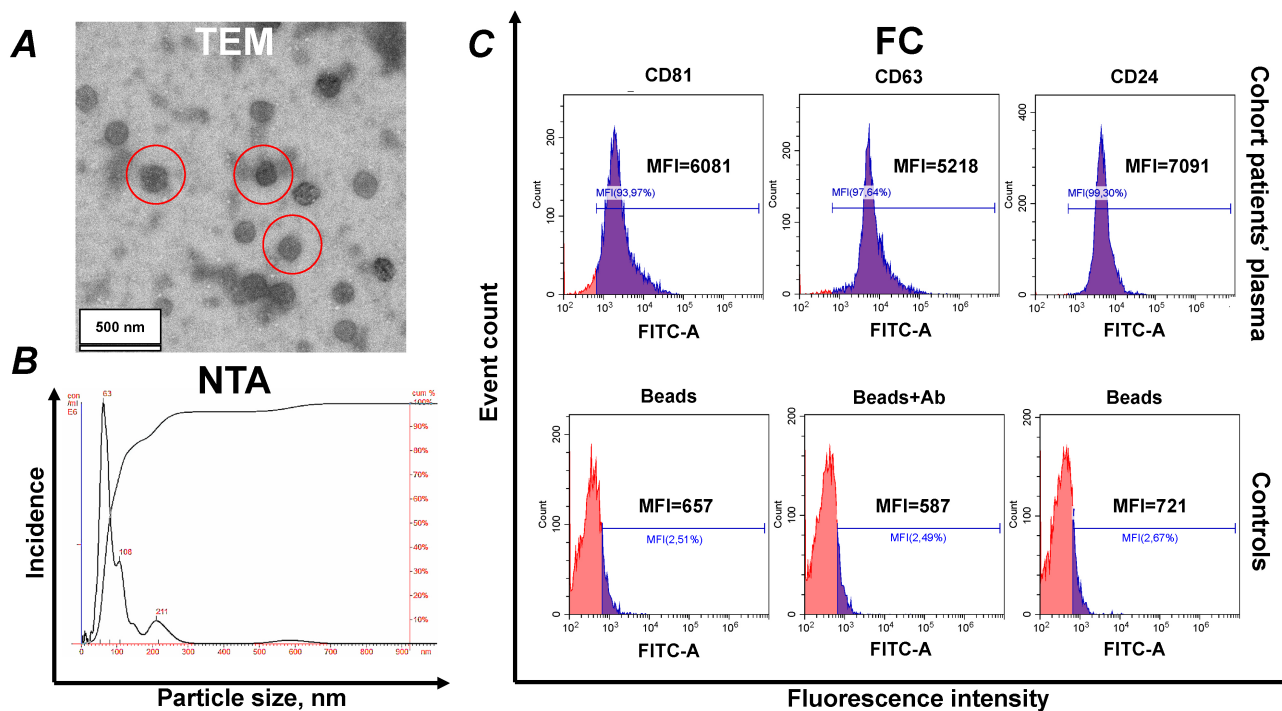


Fig. 2. Identification of isolated sEVs. (A) Electron microscopy, negative staining with phosphotungstic acid ($\times 400$). Red color indicates the non-specific binding. Scale bar = 500 nm. (B) Size distribution of plasma EVs isolated from the blood plasma, data of NTA. (C) Expression of CD81, CD63, and CD24 on CD9-positive EVs of blood plasma. Representative median fluorescence intensity (MFI) values are shown for flow cytometry. Each study was performed in triplicate. For isotype controls (bottom row, histogram at right), labeled CD9 bead-sEV complexes were incubated with mouse FITC IgG1, k Isotype control or mouse FITC IgG2a, or k Isotype control. One of the representative isotypic controls is shown. For the negative control, nothing was added to the CD9 antibody-labeled latex particles (bottom row, histogram at left) or incubated with FITC-labeled anti-human antibodies (anti-CD63, anti-CD81, or anti-CD24) without EVs. One of the representative negative controls is shown (bottom row, histogram in the center). EVs, extracellular vesicles; TEM, transmission electron microscopy; NTA, nanoparticle tracking analysis; FITC, fluorescein isothiocyanate; IgG, immunoglobulin G.

2.4.2 Principal Component Analysis

Additional analyses included posterior probability estimation, correlation analysis, principal component analysis (PCA), and Random Forest modeling. Data visualization was performed using OriginLab and OriginPro 2025b (OriginLab Corporation, Northampton, MA, USA) and R software (version 4.X.X; R Core Team, Vienna, Austria).

3. Results

3.1 Categorical Clinical Signs of the Cohort Patients

Fig. 4 provides a comprehensive view of the posterior probabilities for patients being assigned to one of three diagnostic categories: control, presarcopenia, and sarcopenia. It is based on specific categorical variable values and employs color intensity to represent the magnitude of the probabilities. The probabilities are calculated using empirical frequencies and prior group distributions within the dataset, ensuring that the model's predictions are grounded in the observed data and initial knowledge about the distribution of these categories.

3.2 Description of the Variables

The quantitative parameters of the cohort were divided into four categories: clinical, immunological, vesicular, and biochemical markers (Table 2).

Clinical parameters included general anthropometric indicators and functional assessments related to sarcopenia. The anthropometric indicators comprised age, abdominal circumference, hip circumference, waist-to-hip ratio, BMI, and body fat percentage. Functional and diagnostic markers of sarcopenia included maximal muscle strength, ALM, ASMI, gait speed, total score of SPPB, SARC-F questionnaire score, IPAQ score, SF-36 PH and SF-36 MH components, as well as domains D1–D7 and the total SarQoL.

Immunological markers included the relative proportions of CD14 and CD68 subpopulations of peripheral blood mononuclear cells.

Vesicular markers were represented by the expression levels of MMPs on extracellular vesicles circulating in the blood (characterized by CD9 positivity).

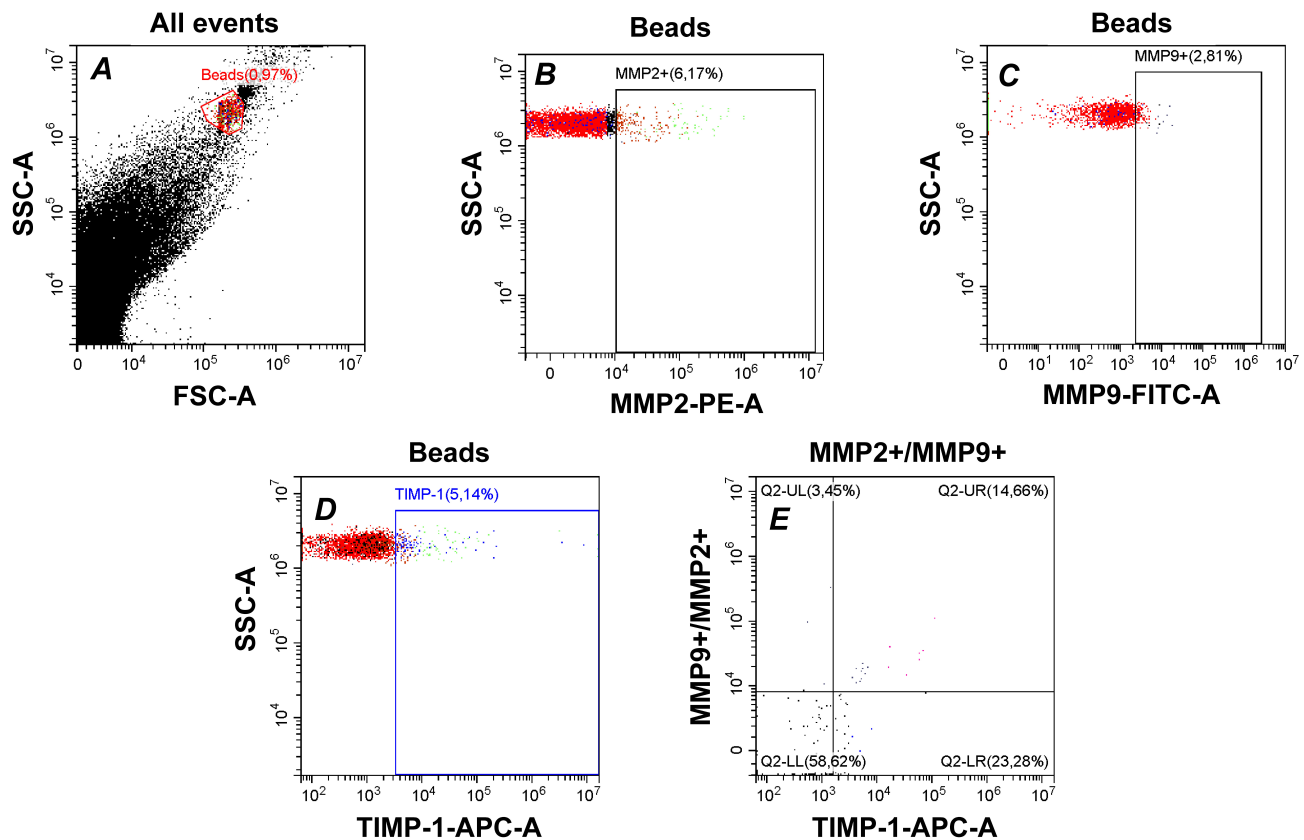


Fig. 3. MMPs subpopulation analysis of extracellular vesicles. (A) Identification of CD9-positive bead-EVs complexes based on forward (FSC-A) and side scatter (SSC-A) light parameters. (B) MMP2-positive EVs within CD9-positive EVs. (C) MMP9-positive EVs within CD9-positive EVs. (D) TIMP-1-positive EVs within CD9-positive EVs. (E) Double staining for MMP2 or MMP9 and TIMP1 is conducted on the subpopulation of EVs negative for MMP2 or MMP9 expression (the choice of MMP2 or MMP9 for double staining is inverted relative to the marker used to define the initially gated MMP2-positive or MMP9-positive EV population) with quadrant gates indicating the proportions of EVs subsets based MMP2/MMP9 and TIMP-1 expression. APC-A, allophycocyanin; FITC-A, fluorescein isothiocyanate; PE-A, phycoerythrin; MMPs, matrix metalloproteinases; TIMP-1, tissue inhibitor of metalloproteinase-1.

Table 2. Clinical and laboratory indicators of cohort patients divided into by groups.

Groups of markers		Indicators
Clinical	Age, Circ. of abdomen, Circ. of hip, Waist/Hip, BMI, Body fat, Max muscle strength, ALM, ASMI, Gait speed, SPPB total, SARC-F, IPAQ, SF-36 PH, SF-36 MH, SarQoL D1-D7, SarQoL total	
Immunological	CD14+163+, CD14-163+, CD14+163-, CD14+163+206-, CD14+163+206+, CD14-163+206+, CD14+163-206+, CD68+163+, CD68-163+, CD68+163-, CD68+163+206+, CD68+163-206+, CD68-163+206+	
Vesicular	MMP9+, TIMP-1, MMP2+, MMP2+9+TIMP+, MMP2+9+TIMP-, MMP2+9-TIMP+, MMP9+2+TIMP+, MMP9+2+TIMP-, MMP9+2-TIMP+	
Biochemical	VTN, Asprosin, METRNL, Glucose, Triglycerides, C-peptide, Elastase-like activity, Trypsin-like activity, α 1-antitrypsin	

BMI, body mass index; ALM, appendicular lean mass; ASMI, appendicular skeletal muscle index; SPPB, Short Physical Performance Battery; SARC-F, sarcopenia screening questionnaire; IPAQ, International Physical Activity Questionnaire; SF-36 PH, SF-36 physical health; SF-36 MH, SF-36 mental health; SarQoL, sarcopenia quality of life; CD, cluster of differentiation; MMP, matrix metalloproteinase; TIMP-1, tissue inhibitor of metalloproteinase-1; VTN, vitronectin; METRNL, meteorin-like protein.

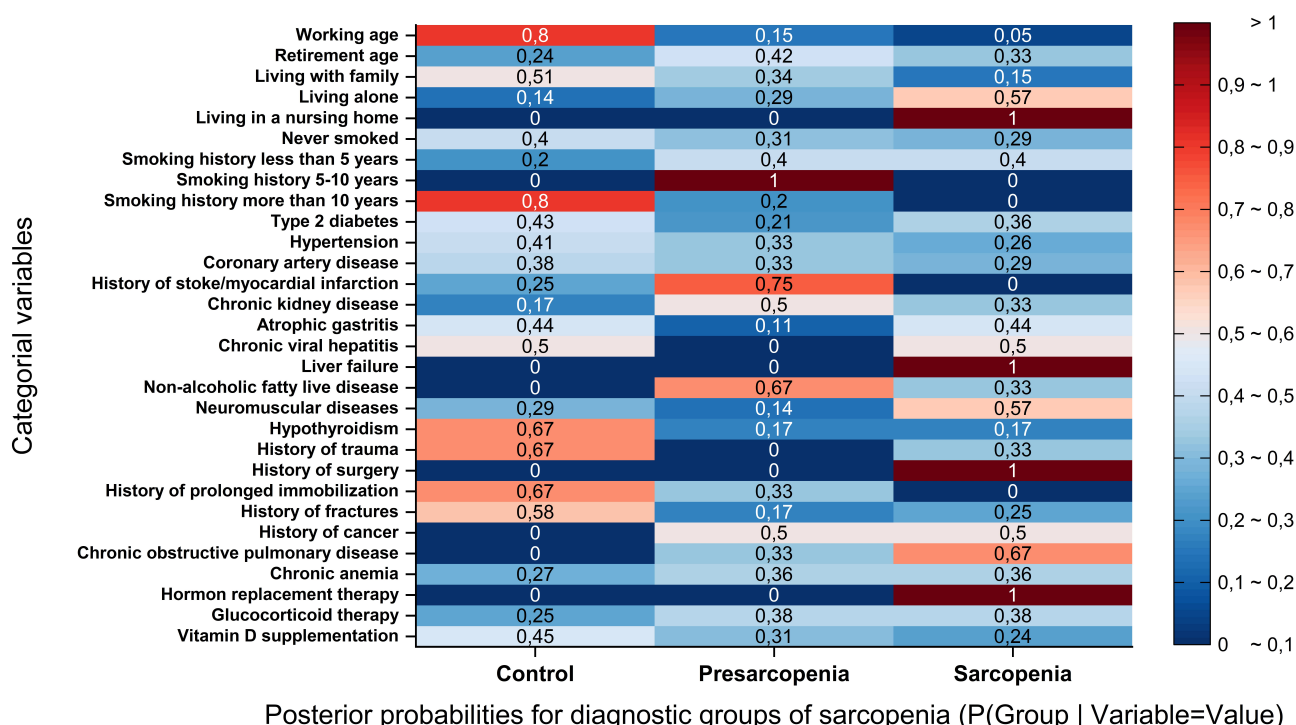


Fig. 4. Posterior probabilities of group membership based on categorical variable states. This heatmap illustrates the posterior probabilities of patient assignment to one of three diagnostic groups (1–control, 2–presarcopenia, 3–sarcopenia) conditional on specific categorical variable values. The y-axis lists variables and their categories (formatted as “variable = value”), while the x-axis represents diagnostic groups. Color intensity corresponds to the magnitude of the posterior probability calculated using empirical frequencies and prior group distributions within the dataset. Warmer colors (orange to red) indicate higher probabilities of group membership given a particular characteristic, whereas lighter tones correspond to lower probabilities. Red color indicates–high probability; light blue–moderate probability and blue–weak probability;

Biochemical markers were classified into three sub-groups:

- (1) Metabolic indicators: glucose, triglycerides, C-peptide.
- (2) Markers of extracellular matrix remodeling: vitronectin (VTN), elastase.
- (3) Sarcopenia-associated markers: asprosin, meteorin-like protein (METRNL), elastase-like activity, trypsin-like activity (TP), α 1-antitrypsin.

3.3 Kruskal–Wallis and Discriminant Analysis Results

Statistical analysis was performed using the Kruskal–Wallis (KW) test for multiple nonparametric quantitative variables. Prior to this, normality was assessed using the Shapiro–Wilk (SW) test, which demonstrated that the distribution of all data deviated from a normal distribution (both within groups and between groups).

Although the SW test indicated significant deviations from normality for several variables, discriminant analysis (DA) was additionally applied to the dataset. In this study, DA was not used exclusively as a method of strict hypothesis testing, but rather as a tool for preliminary evaluation

of the classification potential of individual features. Given that subsequent analyses involve methods such as PCA and Random Forest, which do not require normality assumptions, the use of DA is consistent with the overall strategy aimed at identifying variables with discriminatory power. Deviations from normality, while potentially affecting the precision of classical inferential interpretations in DA, do not critically undermine its practical utility in exploratory and classification-oriented contexts. Discriminant analysis can still provide valuable insight into group separation and variable relevance, even when inferential precision is compromised. Therefore, DA was included as a complementary step to inform feature selection and enhance model interpretability in later stages of the analysis [33–35].

The results of the statistical analysis are presented in Table 3.

In addition to the Kruskal–Wallis test used to assess differences across the three clinical groups (control, presarcopenia, and sarcopenia), pairwise post hoc comparisons were performed using Dunn’s test with Bonferroni correction. The results are presented in Table 4 and allow for clearer interpretation of which specific group differences drive the overall significance observed in the nonparametric tests.

Table 3. Quantitative indicators of patients based on KW-test and discriminant analysis, categorized by groups.

Indicators	Control	Presarcopenia	Sarcopenia	<i>p</i> (SW normality)	<i>p</i> (KW)	<i>p</i> (DA)
Age, years	58 (54; 65)	69.5 (63; 77)	77 (71.75; 80.75)	0.004526	0.000001	0.06083
Circ. of abdomen, sm	94 (84; 106)	93 (87; 104)	86 (83; 87.25)	0.007395	0.003303	0.002647
Circ. of hip, sm	104 (100; 111)	106 (98; 109)	95.5 (92; 100.25)	0.018708	0.000001	0.06883
Waist/Hip, sm	0.9 (0.8; 1)	0.9 (0.8; 0.9)	0.9 (0.8; 0.9)	0.000077	0.933346	0.02325
BMI, units	29.9 (26.5; 30.7)	27.8 (24.3; 33.8)	25.05 (23.55; 26.72)	0.038443	0.001818	0.032022
Body fat, units	24.9 (18.9; 39.3)	27.35 (18; 40.8)	38.2 (34.9; 39.33)	0.000032	0.011510	0.000061
Max muscle strength, units	28 (25; 38)	20 (13; 26)	12.5 (11.5; 15)	0	0.000001	0.113857
ALM, units	18.06 (16.19; 21.42)	17.17 (13.68; 18.6)	13.22 (12.94; 13.93)	0.000005	0.000001	0.041141
ASMI, units	7.02 (6.24; 7.41)	6.89 (5.48; 7.17)	5.48 (5.28; 5.56)	0.00257	0.000001	0.009308
Gait speed, units	0.7 (0.5; 1.13)	0.5 (0.43; 0.89)	0.54 (0.46; 0.66)	0	0.084591	0.166437
SPPB total, units	11 (10; 12)	8.5 (6; 12)	6 (4.75; 8.25)	0	0.000001	0.000015
SARC-F, units	1 (0; 2)	1.5 (0; 3)	3 (1.75; 4.25)	0	0.000202	0.722373
IPAQ, units	25 (17; 32)	25 (19; 38)	19.5 (13.75; 25)	0.000216	0.011270	0.000664
SF-36 PH, units	64 (58; 83.5)	54.5 (34; 72.5)	38.5 (24.6; 47.33)	0.002883	0.000001	0.000016
SF-36 MH, units	62 (47; 78.4)	47.85 (44; 58)	43.45 (34.03; 49.63)	0.00271	0.000001	0.201038
SarQoL D1, units	85.31 (78.54; 89.97)	67 (50.23; 82.19)	53.87 (49.7; 56.88)	0.00002	0.000001	0.217722
SarQoL D2, units	66.51 (57.77; 83.33)	58.68 (52.65; 72.22)	50 (47.92; 63.89)	0.016794	0.002048	0.513579
SarQoL D3, units	65.98 (54.04; 83.33)	54.17 (41.67; 57.58)	52.08 (44.79; 60.62)	0.000032	0.000001	0.532082
SarQoL D4, units	75 (69.37; 88.46)	74.26 (66.47; 80.77)	70.19 (62.5; 76.85)	0.005924	0.041453	0.001259
SarQoL D5, units	68.12 (60.72; 86.54)	59.89 (52.23; 71.67)	61.84 (51.25; 65)	0.007489	0.001151	0.040035
SarQoL D6, units	37.25 (33.25; 48.08)	39.34 (33.25; 53.53)	33.25 (33.25; 48.92)	0.000002	0.297842	0.401493
SarQoL D7, units	87.5 (83.82; 100)	87.5 (78.22; 100)	87.5 (79.11; 87.5)	0	0.041534	0.156659
SarQoL total, units	68.1 (63.46; 83.17)	63.67 (56.48; 72.65)	59.62 (53.19; 63.36)	0.000244	0.000289	0.086097
CD14+163+, %	12.36 (6.51; 16.43)	11.7 (8.18; 13.55)	11.77 (6.7; 16.05)	0.000002	0.843428	0.000178
CD14–163+, %	7.7 (5.24; 10.32)	7.79 (5.78; 10.65)	7.75 (5.88; 11.8)	0.000202	0.891937	0.01277
CD14+163–, %	17.51 (11.54; 23.22)	15.86 (13.78; 19.62)	19.64 (6.43; 33.48)	0.000004	0.767670	0.893563
CD14+163+206–, %	96.56 (95.1; 98.18)	96.43 (94.5; 97.58)	96.15 (93; 98.83)	0.007913	0.742851	0.340369
CD14+163+206+, %	2.82 (1.21; 4.63)	3.37 (2.42; 4.15)	3.85 (1.9; 6.9)	0.020693	0.215716	0.757914
CD14–163+206+, %	4.34 (1.51; 6.33)	2.41 (0.92; 4.76)	5.46 (1.35; 10.12)	0.000021	0.049532	0.045288
CD14+163–206+, %	0.4 (0; 1.49)	0.84 (0; 1.86)	0.31 (0; 0.83)	0.000001	0.545244	0.000994
CD68+163+, %	7.26 (2.89; 10.08)	3.52 (1.61; 10.88)	5.63 (0.97; 12.12)	0.000004	0.713222	0.348318
CD68–163+, %	29.19 (26.29; 36.67)	32.64 (26.81; 41.38)	30.23 (19.59; 46.23)	0.002712	0.717951	0.027512
CD68+163–, %	0.26 (0; 1.34)	0.53 (0.09; 1.28)	0.45 (0.2; 1.66)	0.000001	0.220555	0.674142
CD68+163+206+, %	56.74 (53.07; 62.5)	56.72 (52.21; 62.86)	53.07 (46.95; 58.7)	0.000001	0.212750	0.093227
CD68+163–206+, %	18.38 (8.33; 24.76)	19.55 (5.26; 27.44)	28.09 (4.17; 64.89)	0.000001	0.300672	0.047482
CD68–163+206+, %	4.13 (1.58; 7.87)	5.45 (1.97; 9.26)	5.68 (2.57; 9.61)	0	0.494041	0.263983
MMP9+, %	1.47 (0.78; 3.84)	3.25 (0.38; 5.18)	3.48 (0.89; 4.46)	0	0.676412	0.839688
TIMP-1, %	10.44 (7.86; 13.82)	12 (8.27; 15.11)	11.43 (9.28; 13.15)	0	0.531706	0.03367
MMP2+, %	39.06 (32.82; 46.66)	35.54 (26.45; 44.18)	41.5 (31.59; 47.44)	0.000071	0.386343	0.149164
MMP2+9+TIMP+, %	0.08 (0; 0.49)	0.08 (0; 0.39)	0 (0; 0.24)	0	0.276759	0.237378
MMP2+9+TIMP–, %	1.76 (0.1; 3.24)	1.82 (0.74; 2.92)	1.31 (0.22; 2.55)	0.000003	0.712131	0.086873
MMP2+9–TIMP+, %	10.13 (6.75; 14.15)	11.54 (9.43; 16.21)	10.97 (8.39; 14.61)	0.000378	0.192054	0.277455
MMP9+2+TIMP+, %	12.38 (5.88; 18.08)	12.25 (5.41; 18.39)	12.93 (5.59; 16.08)	0	0.771562	0.644295
MMP9+2+TIMP–, %	13.14 (7.03; 17.13)	13.12 (8.25; 18.98)	13.41 (7.02; 15.26)	0.000042	0.709521	0.627236
MMP9+2–TIMP+, %	13.87 (9.3; 16.11)	15.37 (13.33; 16.84)	16.34 (13.98; 17.56)	0.000518	0.008182	0.007102
VTN (vitronectin), ng/mL	173.38 (141.49; 207.9)	148.3 (100.57; 162.9)	111.6 (95.06; 153.9)	0.000018	0.005263	0.362162
Asprosin, ng/mL	9.97 (6.73; 17.23)	12.36 (8.98; 16.98)	7.89 (6.58; 8.47)	0	0.014851	0.102536
METRNL (meteorin-like protein), ng/mL	1467 (668.5; 2140.25)	1376 (893.1; 1855)	947.05 (392.77; 1202)	0	0.047623	0.054529
Glucose, mM/L	7.44 (6.34; 8.6)	7.62 (5.58; 8.78)	8.84 (6.62; 9.57)	0.001957	0.277275	0.291857

Table 3. Continued.

Indicators	Control	Presarcopenia	Sarcopenia	<i>p</i> (SW normality)	<i>p</i> (KW)	<i>p</i> (DA)
Triglycerides, microM/L	1.55 (1.13; 2.11)	1.55 (1.09; 2.4)	2.26 (1.41; 2.54)	0.019733	0.083976	0.032343
C-peptide, ng/mL	130.2 (74.06; 1058.8)	129.7 (67.77; 852.5)	256.6 (91.42; 908.7)	0	0.568578	0.247876
Elastase-like activity,	177.45 (150.15; 191.1)	191.1 (136.5; 204.75)	163.8 (146.74; 206.97)	0.000236	0.969100	0.004086
Trypsin-like activity, relative units	75.08 (40.95; 107.49)	106.73 (80.19; 150.15)	71.66 (61.42; 156.98)	0	0.017523	0.000595
α 1-antitrypsin, relative units	35.49 (20.22; 43.68)	34.25 (25.36; 42.66)	34.12 (26.28; 44.26)	0.015757	0.818014	0.003037

SW, Shapiro-Wilk; KW, Kruskal-Wallis; DA, discriminant analysis.

3.3.1 Significant Variables According to the KW-Test

The Kruskal-Wallis test, employed due to the non-normal distribution of the data, revealed several variables that significantly differed across study groups ($p < 0.05$). Among clinical markers, age, abdominal and hip circumferences, BMI, body fat percentage, ALM, ASMI, total score on the SPPB, and a number of domains from the SarQoL questionnaire showed significant changes.

From the biochemical indicators, VTN, asprosin, and METRNL demonstrated significant variation. In contrast, vesicular markers, particularly those related to MMP expression, did not reach statistical significance in the KW analysis. Among immunological markers, only the proportion of CD14–CD163+206+ cells exhibited statistically meaningful differences.

In summary, the Kruskal-Wallis test primarily highlighted changes in general clinical status and selected biochemical parameters, while vesicle and immunological markers appeared less sensitive to group differentiation when considered individually.

3.3.2 Pairwise Post Hoc Comparisons Following Kruskal–Wallis Testing

3.3.2.1 Comparison Between Control and Presarcopenia.

In individuals with presarcopenia compared to healthy controls, a statistically significant increase in age was observed (58 → 69.5 years; $p = 0.00082$). Muscle strength significantly decreased (25 → 20 kg; $p = 0.00003$), along with a reduction in ALM (18.07 → 13.68 kg; $p = 0.01618$) and ASMI (7.02 → 5.87 units; $p = 0.02582$). Quality of life in the physical domain significantly declined, as reflected by lower scores in the SF-36 Physical Health component (64 → 54.25 units; $p = 0.0126$) and SarQoL domain D1 (89.2 → 72.2; $p = 0.00119$). Additionally, vitronectin levels significantly decreased (173.8 → 148.0 ng/mL; $p = 0.03598$), as did trypsin-like protease activity (75.08 → 74.12 units; $p = 0.00671$).

3.3.2.2 Comparison Between Control and Sarcopenia.

Compared to controls, participants with sarcopenia exhibited a significant increase in age (58 → 77 years; $p < 0.00001$) (Table 4). Significant reductions were detected in abdominal circumference (94 → 87 cm; $p = 0.00117$), hip circumference (93 → 87 cm; $p < 0.00001$), BMI (24.2

→ 22.2 kg/m²; $p = 0.00069$), body fat content (34.2 → 27.3 units; $p = 0.01013$), muscle strength (25 → 12.5 kg; $p < 0.00001$), ALM (18.07 → 12.94 kg; $p = 0.00259$), and ASMI (7.02 → 5.25 units; $p = 0.00807$). Functional capacity, measured by total SPPB score, also declined markedly (11 → 6 points; $p = 0.00013$).

Health-related quality of life was significantly lower in sarcopenic patients, including scores for SF-36 PH (64 → 24.67 units; $p = 0.00001$), SarQoL D1 (89.2 → 58.2; $p = 0.00001$), D2 (85.6 → 62.8; $p = 0.00101$), D3 (79.2 → 64.8; $p = 0.00174$), D4 (82.4 → 57.2; $p = 0.01916$), D5 (81.6 → 61.6; $p = 0.0015$), and overall SarQoL total score (88.2 → 65.7; $p = 0.00019$).

Among biochemical markers, vitronectin levels significantly decreased (173.8 → 111.6 ng/mL; $p = 0.00416$), as did asprosin (9.32 → 6.58 ng/mL; $p = 0.04956$) and METRNL (1376 → 692 pg/mL; $p = 0.0578$). Though the last two changes are borderline, they reflect a clear downward trend.

3.3.2.3 Comparison Between Presarcopenia and Sarcopenia.

In the transition from presarcopenia to sarcopenia, age significantly increased (69.5 → 77 years; $p = 0.0295$). Anthropometric parameters also declined: abdominal circumference (93 → 87 cm; $p = 0.023$), hip circumference (90 → 87 cm; $p = 0.00024$), BMI (23.9 → 22.2; $p = 0.01067$), and body fat (30.1 → 27.3 units; $p = 0.01047$). ALM (13.68 → 12.94 kg; $p = 0.00259$) and ASMI (5.87 → 5.25; $p = 0.00807$) continued to decrease.

A further decline was seen in SarQoL D1 scores (72.2 → 58.2; $p = 0.04286$). Inflammatory/metabolic markers also showed deterioration: asprosin levels (9.32 → 6.58 ng/mL; $p = 0.00606$) and METRNL (853 → 692 pg/mL; $p = 0.03432$) both significantly decreased.

The direction and magnitude of changes were evaluated by comparing median values across the groups (see Table 3), while statistical significance for each comparison is reported in Table 4.

3.3.3 Variables Identified Through Discriminant Analysis

In parallel, DA was conducted to explore the classification potential of the study variables. Here, the list of significant predictors shifted slightly. DA indicated that waist-to-hip ratio, BMI, body fat content, ALM, ASMI, to-

Table 4. Post hoc pairwise comparisons using Dunn's test (with Bonferroni correction) between clinical groups (Control – 1, Presarcopenia – 2, Sarcopenia – 3).

Indicators	<i>p</i> (KW)	<i>p</i> (Dunn) 1 vs 2	<i>p</i> (Dunn) 1 vs 3	<i>p</i> (Dunn) 2 vs 3
Age, years	0.000001	0.00082	0	0.0295
Circ. of abdomen, sm	0.003303	0.55683	0.00117	0.023
Circ. of hip, sm	0.000001	0.60694	0	0.00024
Waist/Hip, sm	0.933346	1	1	1
BMI, units	0.001818	0.69517	0.00069	0.01067
Body fat, units	0.011510	1	0.01013	0.01047
Max muscle strength, units	0.000001	0.00003	0	0.01412
ALM, units	0.000001	0.01618	0	0.00259
ASMI, units	0.000001	0.02582	0	0.00807
Gait speed, units	0.084591	0.13786	0.07361	0.97208
SPPB total, units	0.000001	0.00138	0.00013	0.5164
SARC-F, units	0.000202	0.29101	0.00006	0.0076
IPAQ, units	0.011270	0.86027	0.01723	0.00659
SF-36 PH, units	0.000001	0.0126	0	0.00435
SF-36 MH, units	0.000001	0.00776	0.00001	0.09402
SarQoL D1, units	0.000001	0.00119	0	0.04286
SarQoL D2, units	0.002048	0.05435	0.00101	0.2135
SarQoL D3, units	0.000001	0.00007	0.00174	1
SarQoL D4, units	0.041453	0.29216	0.01916	0.30562
SarQoL D5, units	0.001151	0.00919	0.0015	0.61153
SarQoL D6, units	0.297842	1	0.28622	0.20705
SarQoL D7, units	0.041534	0.25588	0.02006	0.3485
SarQoL total, units	0.000289	0.01501	0.00019	0.20771
CD14+163+, %	0.843428	0.96757	0.92266	1
CD14–163+, %	0.891937	1	0.99473	1
CD14+163–, %	0.767670	0.94273	1	0.71759
CD14+163+206–, %	0.742851	1	0.67002	0.84249
CD14+163+206+, %	0.215716	0.63365	0.12201	0.4928
CD14–163+206+, %	0.049532	0.18188	0.36549	0.02569
CD14+163–206+, %	0.545244	0.40651	1	0.85955
CD68+163+, %	0.713222	0.62442	1	1
CD68–163+, %	0.717951	0.65664	0.91015	1
CD68+163–, %	0.220555	0.49747	0.13406	0.63947
CD68+163+206+, %	0.212750	1	0.1581	0.1776
CD68+163–206+, %	0.300672	1	0.19782	0.322
CD68–163+206+, %	0.494041	0.94817	0.35301	0.7062
MMP9+, %	0.676412	0.72531	0.67117	1
TIMP-1, %	0.531706	0.39333	0.93926	0.95654
MMP2+, %	0.386343	0.42211	1	0.30402
MMP2+9+TIMP+, %	0.276759	0.68169	0.16657	0.56732
MMP2+9+TIMP–, %	0.712131	0.80016	1	0.65927
MMP2+9–TIMP+, %	0.192054	0.10393	0.76138	0.56637
MMP9+2+TIMP+, %	0.771562	1	0.75682	0.78941
MMP9+2+TIMP–, %	0.709521	1	0.80431	0.61935
MMP9+2–TIMP+, %	0.008182	0.05197	0.00582	0.49868
VTN (vitronectin), ng/mL	0.005263	0.03598	0.00416	0.51555
Asprosin, ng/mL	0.014851	0.44424	0.04956	0.00606
METRNL (meteorin-like protein), ng/mL	0.047623	1	0.0578	0.03432
Glucose, mM/L	0.277275	1	0.17923	0.30012
Triglycerides, microM/L	0.083976	1	0.04686	0.10682
C-peptide, ng/mL	0.568578	1	0.54083	0.47616
Elastase-like activity,	0.969100	1	1	1
Trypsin-like activity, relative units	0.017523	0.00671	0.49552	0.22446
α1-antitrypsin, relative units	0.818014	1	0.811	0.90743

METRNL, meteorin-like protein.

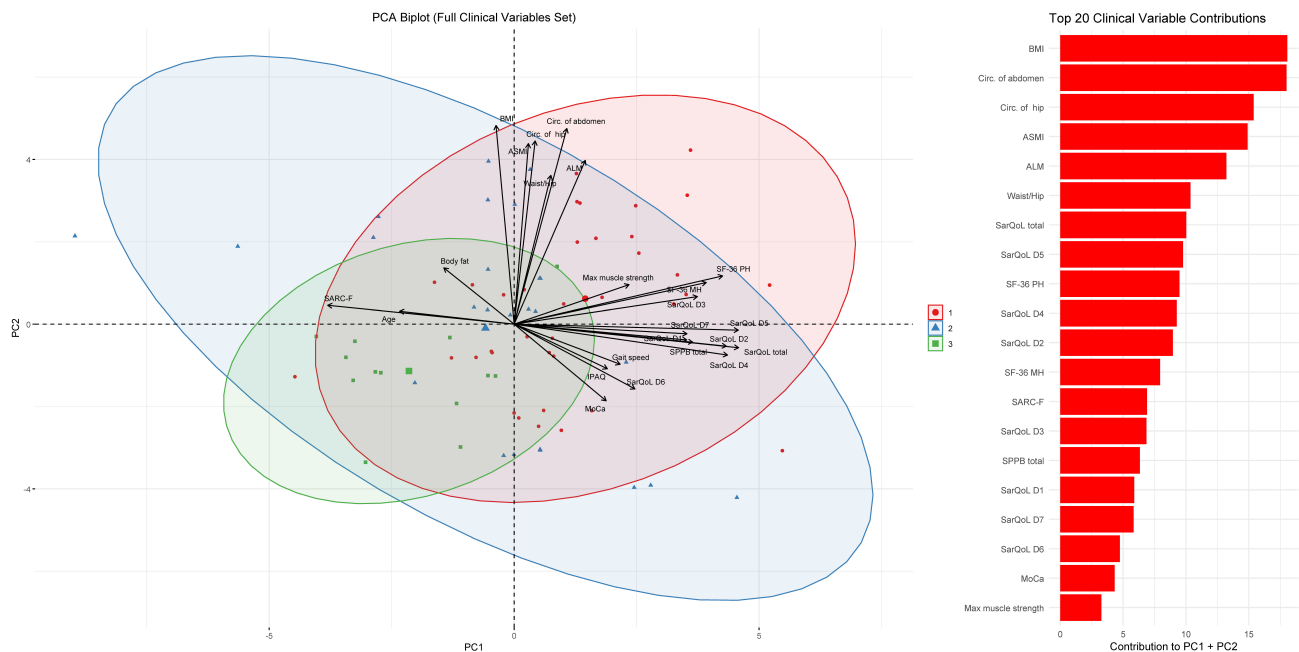


Fig. 5. Principal component analysis (PCA) biplot of clinical characteristics related to sarcopenia progression. The biplot displays the first two principal components (PC1 and PC2), summarizing the largest part of variability among clinical parameters. Each point corresponds to an individual subject and is color-coded according to clinical group assignment: control (1), presarcopenia (2), or sarcopenia (3). The x-axis (PC1) and y-axis (PC2) represent the orthogonal dimensions capturing the main patterns of variation. Arrows indicate the contributions of clinical variables to the principal components; the direction and length of each arrow reflect the strength and orientation of the corresponding variable's influence. The dispersion and grouping of points, as well as the vector distribution, suggest clinical differentiation among groups along the principal components. To the right of the biplot, a barplot displays the top 20 clinical variables contributing to the total variance explained by PC1 and PC2. The variables are ranked by their combined contribution and help highlight the most influential factors underlying group separation.

tal SPPB score, IPAQ, the SF-36 Physical Health component, and several SarQoL domains (D4, D5) were influential in distinguishing between groups.

Notably, DA also brought to light immunological markers that the Kruskal–Wallis test had overlooked, including CD14+CD163+, CD14–CD163+, CD68–CD163+, and CD68+CD163–206+. Vesicular markers such as TIMP-1, as well as biochemical variables like triglycerides, elastase-like activity, trypsin-like activity, and α 1-antitrypsin, also contributed meaningfully to classification according to DA.

Discriminant analysis revealed that several markers, even those lacking strong univariate differences, exhibited meaningful classification ability. This indicates their potential use as predictive features for sarcopenia diagnosis and progression modeling, warranting further validation in larger cohorts.

3.4 Principal Component Analysis of the Data

3.4.1 Principal Component Analysis (PCA)

PCA was performed on the two groups of following quantitative variables. First group included clinical variables and the second one — immunological, vesicular and metabolic data. The grouping variable was the

disease status (control, presarcopenia, sarcopenia) (Fig. 5). Variables were standardized and missing data were removed. Feature space was orthogonalized into components with calculation of variance explained by each component. PCA was used to explore the structure of relationships among inflammation markers, extracellular matrix degradation markers, and metabolic indicators across different sarcopenia stages. Unlike univariate methods such as the Kruskal–Wallis test, PCA can capture complex interdependencies between variables and identify major axes of variation without prespecifying group memberships, thus better reflecting underlying biological processes. Methodologically, the use of PCA in this study was justified, as it enabled not only the identification of differences between groups based on individual markers but also the reconstruction of the complex biological landscape of sarcopenia's markers [36].

The PCA performed on 24 clinical variables revealed key dimensions of variability in the cohort. Principal Component 1 (PC1) and Principal Component 2 (PC2) accounted for 32.03% and 19.26% of the total variance, respectively. The cumulative variance explained by the first five components reached 73.94%, indicating a high dimensional structure typical for sarcopenia-related clinical data.

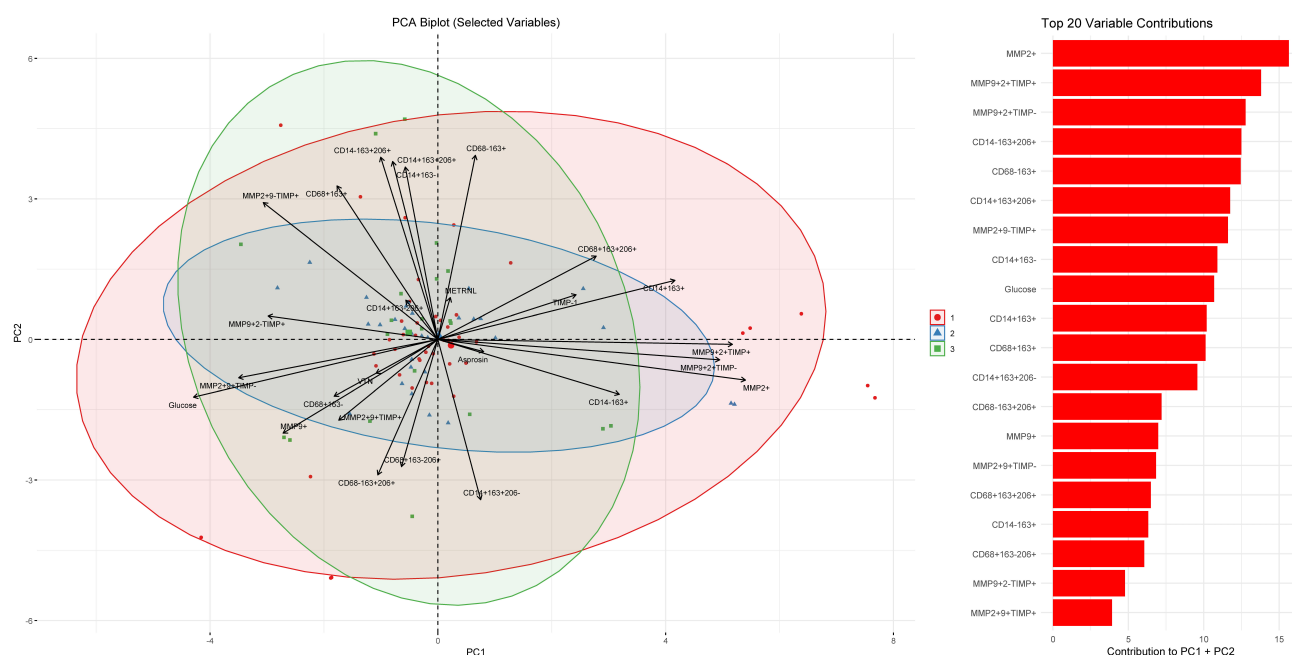


Fig. 6. Principal component analysis (PCA) biplot of laboratory markers related to sarcopenia development. The plot presents the first two principal components (PC1 and PC2), (x-axis is for PC1 and y-axis is for PC2) explaining the major portion of variance within the dataset. Each point represents an individual participant, colored according to the clinical group: control (1), presarcopenia (2), and sarcopenia (3). Vectors indicate the loadings of laboratory markers, with their directions and lengths reflecting their contribution to the principal components. Markers closely aligned with the axes contribute strongly to the corresponding component. The clustering of individuals and the spatial distribution of vectors suggest distinct biomarker profiles across groups, highlighting potential biological gradients associated with sarcopenia progression. To the right of the biplot, a barplot displays the top 20 laboratory variables contributing to the total variance explained by PC1 and PC2. The variables are ranked by their combined contribution and help highlight the most influential factors underlying group separation.

All variables were centered and scaled prior to analysis. A full breakdown of explained variance is provided in **Supplementary Table 1**. These components were selected for biplot visualization due to their maximal contribution to sample separation and interpretability (**Supplementary Table 2**).

The first principal component (PCA1) showed the highest factor loadings for variables reflecting the anthropometric characteristics of the participants (circumference of abdomen, circumference of hip, waist-to-hip ratio) and skeletal muscle status (appendicular lean mass, appendicular skeletal muscle index). These parameters decreased with sarcopenia progression and demonstrated a positive correlation with BMI, which also contributed significantly to PCA1.

The second principal component (PCA2) was primarily defined by age, patient-reported quality of life (as assessed by the Sarcopenia Quality of Life questionnaire domains D1, D2, D3, D4, D5, D7 and total score; SARC-F score; and SF-36 physical and mental health components), and functional capacity (maximal muscle strength, Short Physical Performance Battery). Disease severity showed a positive correlation with patient age and the SARC-F score, a trend most evident in the control and sarcopenia groups.

Body fat percentage did not contribute to either PCA1 or PCA2. However, it was strongly negatively correlated with physical activity level (International Physical Activity Questionnaire), gait speed, and Domain 6 of the SarQoL questionnaire, which reflects patients' leisure activity.

The presented PCA biplot confirms a fundamental relationship between patients' quality of life and sarcopenia severity and reveals bidirectional associations between these clinical characteristics and functional status (Fig. 6).

The PCA performed on 26 laboratory markers allowed for the identification of key biochemical, immunological, and metabolic features characterizing the transition from normal status to presarcopenia and sarcopenia. PC1 and PC2 explain 18.28% and 11.90% of the total variance, respectively. The total variance explained by the first two components is 30.18%. All variables were standardized prior to analysis (centered and scaled). Although this level of explained variance is moderate, it reflects the biological heterogeneity of the cohort and is typical for high-dimensional clinical datasets. A full breakdown of variance explained by each component is provided in **Supplementary Table 1**. The use of the complete set of variables and a careful analysis of their localization on the biplot and their contributions to PC1 and PC2 provided a more comprehen-

sive understanding of the underlying pathogenic processes (**Supplementary Table 2**).

The first principal component (PC1) mainly reflected changes associated with enhanced inflammation, activation of matrix metalloproteinases, and ECM degradation. High contributions to PC1 were made by markers of ECM destruction (MMP9+, MMP2+, MMP2+9+TIMP+, MMP9+2–TIMP+), as well as by inflammatory macrophage subpopulations (CD68+163–206+, CD14–163+). These findings indicate the progressive remodeling of tissues and chronic inflammation correlated with the severity of sarcopenia.

The second principal component (PC2) emphasized differences associated with metabolic disturbances (Glucose, asprosin, triglycerides) and changes in macrophage activation profiles (e.g., CD68+163+, CD14+163+), reflecting compensatory or transitional processes that are particularly prominent at the presarcopenia stage.

3.4.2 PCA Data Clustering

Functional clustering of markers, based on their contribution to PC1/PC2 and spatial distribution on the biplot, allowed for the identification of four key groups.

3.4.2.1 Extracellular Matrix Degradation Cluster. This cluster includes MMP2+, MMP9+, MMP2+9+TIMP+, MMP2+9+TIMP–, MMP9+2–TIMP+, MMP9+2+TIMP–, and TIMP-1 as a metalloproteinase inhibitor. Their vectors were predominantly directed into the first and second quadrants, and a positive correlation was noted between metalloproteinase activity and sarcopenia progression. The increased expression of these markers accompanies the transition from healthy status to sarcopenia, reflecting ECM destruction and insufficient regulatory control.

3.4.2.2 Inflammation and Macrophage Activation Cluster. This group includes markers such as CD14–163+, CD14+163–, CD14–163+206+, CD68–163+, CD68–163+206+, and CD68+163–206+, representing inflammatory macrophage activation. Their contribution to PC1 is particularly significant, and their vectors are also directed mainly toward the first and second quadrants. This indicates that inflammatory response and tissue destructive processes are closely linked and progressively intensify in sarcopenia.

3.4.2.3 Homeostasis and Stabilization Cluster. This cluster includes CD14+163+, CD68+163+, CD14+163+206+, CD68+163+206+, and MMP9+2+TIMP+. These markers demonstrate smaller contributions to PC1 and moderate contributions to PC2, with vectors localized near the center of the biplot, corresponding to the control group. Their presence indicates preserved tissue homeostasis and a balance between degradation and remodeling, characteristic of healthy tissues.

3.4.2.4 Metabolic Disturbance Cluster. This group consists of glucose, asprosin, triglycerides, C-peptide, METRN, and TP. Their contributions are more prominent along the PC2 axis, and their vector direction reflects energy metabolism disturbances characteristic of late-stage sarcopenia. Increased glucose and adipokine levels, along with disrupted lipid metabolism, indicate systemic metabolic changes associated with muscle mass and function loss.

Special attention should be given to α 1-antitrypsin, a marker of acute-phase inflammation, which is located within the region of active inflammatory response, confirming its involvement in sarcopenia pathogenesis. Elastase and VTN also contribute to tissue remodeling processes, emphasizing the importance of the imbalance between ECM destruction and regeneration.

Integration of PCA results demonstrated that the control group is characterized by the predominance of stabilizing macrophage profiles, moderate metalloproteinase activity, and preserved metabolic reserve capacity. In the early stages of sarcopenia, there is a noticeable rise in the activity of metalloproteinases, chronic inflammation, and significant metabolic disturbances (Table 5, Ref. [6–32]).

4. Discussion

4.1 Comprehensive Study of Biochemical, Immunological, and Metabolic Markers: Fundamentals and Relationships

4.1.1 Limitations Related to Study Design and Statistical Interpretation

The authors acknowledge several limitations related to the study design and statistical methodology, which should be considered for a balanced interpretation of the findings. The cross-sectional nature of the study does not allow for definitive conclusions about causality. The patterns of biomarkers distribution were associated with sarcopenia severity, it remains unclear whether these changes are primary causes, compensatory mechanisms, or secondary effects. The prospective follow-up over 6–12 months is warranted to assess the dynamics and prognostic value of these indicators.

The patient stratification was performed according to the EWGSOP2 criteria, the practical implementation of these criteria (e.g., the handgrip strength measurement protocol, ASMI calculation using bioimpedance analysis, and threshold values for low muscle mass and strength) requires further standardization to enhance reproducibility and external validity.

One of the key limitations of this study is the relatively small and uneven sample size across defined subgroups. In particular, gender-stratified subgroups occasionally included as few as two individuals, which limits the statistical power for detecting subtle differences and increases the risk of type II error. The resulting imbalance should be considered when interpreting group-wise comparisons, especially in exploratory analyses involving immune or vesicular ma-

Table 5. Results of principal component analysis (PCA) for laboratory indicators, including principal component coefficients, group categorization, biological interpretation, vector orientation, and type of correlation with principal components.

Laboratory indicator	PC1 coefficient	PC2 coefficient	Contribution to PC1 (%)	Contribution to PC2 (%)	Total contribution (%)	Quadrant	Correlation type	Interpretation	Link source
CD14+163+	−0.20367	−0.1296	5.9	2.32	8.22	III	positive	Anti-inflammatory macrophages, typical for control group.	[6]
CD14−163+	0.084272	0.119334	1.01	1.96	2.97	I	positive	Activation of inflammatory macrophages, increases with sarcopenia.	[7,8]
CD14+163−	−0.1891	0.039169	5.08	0.21	5.3	II	negative	Transitional macrophage profile, initial inflammatory activation.	[9–11]
CD14+163+206−	0.033763	0.301404	0.16	12.53	12.7	I	positive	Moderately activated macrophages, early changes in sarcopenia.	
CD14−163+206+	−0.01947	0.240272	0.05	7.96	8.02	II	negative	Inflammatory macrophages associated with tissue destruction.	
CD14+163−206+	−0.00783	0.280749	0.01	10.87	10.88	II	negative	Transition to inflammation, onset of ECM remodeling.	
MMP9+	0.105089	0.233195	1.57	7.5	9.07	I	positive	Active ECM degradation, sarcopenia.	[12]
TIMP-1	−0.09703	−0.21475	1.34	6.36	7.7	III	positive	Metalloproteinase inhibitor, imbalance in sarcopenia.	[13]
MMP2+	0.049124	0.257751	0.34	9.17	9.51	I	positive	Connective tissue destruction, activated in sarcopenia.	[14–18]
MMP2+9+TIMP+	−0.11119	−0.00665	1.76	0.01	1.76	III	positive	Complex ECM remodeling imbalance.	
MMP2+9+TIMP−	0.099876	−0.03559	1.42	0.17	1.59	IV	negative	ECM destruction without inhibitory control.	
MMP2+9−TIMP+	−0.209	−0.01623	6.21	0.04	6.25	III	positive	Controlled MMP activation, typical for presarcopenia.	
MMP9+2+TIMP+	0.220789	−0.01712	6.93	0.04	6.97	IV	negative	Balanced ECM degradation, transitional phase.	
MMP9+2+TIMP−	−0.20037	0.031233	5.71	0.13	5.84	II	negative	Enhanced ECM destruction, sarcopenia.	
MMP9+2−TIMP+	0.109235	−0.05606	1.7	0.43	2.13	IV	negative	Active ECM destruction, late-stage sarcopenia.	
VTN	0.130897	−0.12311	2.44	2.09	4.53	IV	negative	Vitronectin, modulation of cell adhesion, decreased in sarcopenia.	[19,20]
Asprosin	0.202931	0.104386	5.85	1.5	7.36	I	positive	Regulator of glucose metabolism, increased in sarcopenia.	[21,22]
METRNL	0.16293	0.109547	3.77	1.66	5.43	I	positive	Myokine response to inflammation, possible compensatory mechanism.	[23]
Glucose	0.19243	−0.0076	5.26	0.01	5.27	IV	negative	Glucose metabolism disturbance, associated with sarcopenia.	[24,25]
Triglycerides	0.192231	−0.00294	5.25	0	5.25	IV	negative	Dyslipidemia, metabolic component of sarcopenia.	[26]
C-peptide	0.159222	0.077288	3.6	0.82	4.43	I	positive	Indicator of insulin secretion, impaired in sarcopenia.	[27]
Elastase-like activity	0.192222	−0.02785	5.25	0.11	5.36	IV	negative	Destruction of elastic fibers, tissue remodeling.	[28,29]
Trypsin-like activity	0.208311	0.023308	6.17	0.07	6.24	I	positive	Total protein, general nutritional status, decreased in sarcopenia.	[30,31]
α1-antitrypsin	0.100607	−0.0813	1.44	0.91	2.35	IV	negative	Acute phase inflammation, activated in sarcopenia.	[32]

rkers. Small sample size ($n = 55$) can limit the statistical power, particularly in multivariate analyses. PCA was used as an exploratory tool to identify biological gradients; however, clusters observed in biplots were interpreted visually and were not statistically validated using formal tests such as PERMANOVA. These facts may create a risk of overinterpreting visually apparent group separations and underscores the need for replication in larger cohorts.

Furthermore, no adjustments were made for potential confounding factors. Variables such as age, body mass index, and chronic conditions (e.g., diabetes mellitus and chronic kidney disease) can influence both metabolic and inflammatory markers. Their effects may overlap with or obscure sarcopenia-specific processes. Future analyses should incorporate multivariate approaches, such as generalized linear models (GLMs), to evaluate independent associations with sarcopenia status.

Although PCA enabled visualization of marker clusters and gradients, it has interpretational limitations. Variables that differed significantly between groups in univariate tests (e.g., METRNL) made only minor contributions to the first two principal components. Therefore, PCA results should be interpreted in conjunction with supervised methods and univariate statistics.

Finally, discriminant analysis and PCA helped to identify several potentially informative biomarkers, a complete diagnostic model was not developed in the current study. Receiver Operating Characteristic (ROC) analysis and Least Absolute Shrinkage and Selection Operator (LASSO) regression were not performed, and diagnostic cut-off values were not proposed. These steps are necessary to evaluate the clinical utility of the markers and should be included in future research.

In summary, the cross-sectional design, limited sample size, and lack of certain statistical adjustments call for cautious interpretation. Longitudinal, statistically robust studies with larger samples are required to validate the observed patterns and to develop reliable diagnostic and prognostic models.

4.1.2 Flow Cytometry Analysis of Mononuclear Cells

Naturally, despite the many advantages of flow cytometry, both in the typing of mononuclear cells and in the subpopulation analysis of EVs protein markers, several limitations of the method must be acknowledged. Common issues include nonspecific staining, spectral overlap of fluorescent labels (necessitating compensation), and the instability of antibody-protein complexes, both on the surface of cells and on EVs surfaces [33]. For cell-based assays, there is also the problem of accurately representing subpopulation ratios due to cell disruption during sample preparation and pre-analytical handling. In the case of EVs analysis, staining procedures involve the additional challenge of unstable adsorption of EVs onto latex beads.

Other important limitations include background noise caused by antibody aggregates or unbound fluorophores, the potential for epitope masking due to conformational changes or competitive binding, and a general difficulty in detecting low-abundance markers owing to the small surface area of EVs. Furthermore, flow cytometry analysis of EVs is inherently limited by the instrument's detection threshold, leading to the exclusion of small-sized vesicles or the misclassification of EVs subtypes.

As a result, truly accurate evaluation of immunological and vesicular markers requires further methodological refinement and the incorporation of complex correction strategies. Nevertheless, certain intrinsic limitations—such as physical detection limits, antibody specificity, and pre-analytical variability—will inevitably continue to distort the true results of the analysis, regardless of technical improvements.

4.1.3 Interpretation of Vesicular Marker Results

The role of MMPs and their tissue inhibitor (TIMP-1) undoubtedly reflects ECM remodeling, a central component in the pathogenesis of sarcopenia. In our study, MMP2, MMP9, and TIMP-1 were assessed on the surface of CD9-positive EVs derived from the general circulation [17,34]. Although individual comparisons between clinical groups did not reach statistical significance in univariate analyses (e.g., Kruskal–Wallis test), these vesicular markers contributed substantially to the PC1, which aligned with clinical severity and grouped inflammatory and matrix-remodeling variables. This suggests that, despite limited univariate discrimination, EV-associated MMPs carry multivariate value in the biological stratification of sarcopenia [17,35].

However, the examination of these vesicular markers in the aggregate EV populations is limited by a lack of tissue-specificity. The observed differences may be attributed to the variations in clinical characteristics between the groups, such as age and body mass index. This is particularly true for markers that are linked to multiple age-related conditions, including inflammation, metabolic processes, mitochondrial function, and extracellular matrix remodeling. The detection of MMPs on CD9+ EVs may represent a generalized picture of ECM remodeling within the organism, including signals from diverse tissues such as vascular endothelium, adipose tissue, or smooth muscle. Therefore, while informative in a systems biology context, this approach cannot distinguish muscle-specific remodeling events from systemic matrix turnover [36].

To address this limitation, future approaches should focus on identifying a reliable skeletal muscle-specific marker detectable on circulating EVs. Such a marker should ideally be associated with structural or contractile proteins specific to muscle fibers or their resident cells—e.g., desmin, titin, myosin heavy chains, or caveolin-3 [37–40]. The detection of EVs co-expressing MMPs and

muscle-specific proteins would allow for more precise attribution of matrix remodeling to skeletal muscle, rather than other tissues undergoing parallel degeneration or remodeling processes.

Moreover, the need to differentiate skeletal muscle-derived EVs from those of smooth muscle and cardiac origin remains critical. Both vascular and myocardial remodeling can influence the EV cargo profile, particularly under conditions common in older adults, such as hypertension, atherosclerosis, or heart failure. Misattributing such vesicles to skeletal muscle could lead to erroneous conclusions regarding sarcopenia-specific processes. Incorporating muscle-specific EV markers, possibly in combination with transcriptomic or proteomic validation, will be essential to improving diagnostic and prognostic utility in sarcopenia research.

4.1.4 Interpretation of Biochemical Marker Results

The interpretation of biochemical and immunological markers provides essential insights into the biological mechanisms underpinning sarcopenia progression. Our data support stage-specific trajectories of change, reflected both in median values and in statistically significant post hoc differences.

Among metabolic indicators, asprosin and METRNL demonstrated statistically significant increases across disease stages. Asprosin levels rose in serum from a median of 1.35 in controls to 1.74 in sarcopenia ($p = 0.0036$), while METRNL increased from 1.08 to 1.34 ($p = 0.0067$), indicating possible roles in energy mobilization and muscle regeneration. Vitronectin (VTN) levels decreased between presarcopenia and sarcopenia (medians 5.12 vs. 3.55; $p = 0.0041$), suggesting progressive disruption in extracellular matrix homeostasis.

Proteolytic enzyme activity markers showed consistent changes: elastase increased from control to presarcopenia (0.85 vs. 1.15; $p = 0.0348$), remaining elevated in sarcopenia (1.15). Similarly, trypsin-like proteolytic activity (TP) rose from 0.86 to 1.19 ($p = 0.0139$), indicating enhanced proteolytic stress during early and mid-stage muscle decline.

Among immunological variables, the CD14–CD163+CD206+ monocyte population exhibited a U-shaped dynamic: a significant decrease in presarcopenia compared to control (6.6 vs. 4.6; $p = 0.03598$), followed by a moderate increase in sarcopenia (6.2). This non-linear trend may reflect transient depletion of anti-inflammatory M2-like monocytes in early decline, with partial restoration in advanced disease. Additionally, significant differences were observed for CD68+CD163+, CD14+CD163+, and CD68–CD163+ populations, with decreased levels in sarcopenia relative to control or presarcopenia, supporting the hypothesis of altered monocyte/macrophage polarization along the sarcopenia trajectory.

These patterns are quantitatively supported by both median comparisons (Table 3) and post hoc significance (Table 4). Together, they indicate a progressive inflammatory and proteolytic shift during disease development, involving specific monocyte subsets and circulating biochemical regulators.

4.2 Complex Validation of Sarcopenia Pathogenesis

4.2.1 Inflammation and ECM Remodeling

Inflammation plays a crucial role in the pathogenesis of sarcopenia, contributing to muscle loss and dysfunction. Chronic low-grade inflammation, often observed in aging, can lead to the release of pro-inflammatory cytokines, which in turn can impair muscle protein synthesis and promote muscle catabolism [3]. Additionally, inflammation can affect the ECM remodeling process. The ECM provides structural support and plays a key role in muscle repair and regeneration. Dysregulation of ECM remodeling, characterized by altered expression of MMPs and their inhibitors (TIMPs), can disrupt the balance between muscle degeneration and regeneration, further exacerbating muscle loss in sarcopenia [41].

Sarcopenia is characterized by progressive muscle mass, strength, and function loss, often linked to aging. Recent research emphasizes the roles of chronic inflammation and proteolytic dysregulation in its development.

Immunological markers, notably CD14–CD163+206+ cells, show significant deviations in sarcopenia, indicating a chronic inflammatory state. These cells suggest an ongoing inflammatory response contributing to muscle tissue degradation. Proteolysis markers also impact ECM remodelling. Elastase-like, trypsin-like activities, and $\alpha 1$ -antitrypsin are involved in pre-sarcopenia and sarcopenia, breaking down ECM proteins and leading to muscle tissue degradation and function loss.

Chronic inflammation, proteolytic dysregulation, and metabolic perturbations are interconnected. Inflammation releases pro-inflammatory cytokines, activating proteolytic pathways and disrupting metabolism. Proteolytic dysregulation breaks down muscle proteins, while metabolic perturbations affect energy production and nutrient utilization.

Understanding sarcopenia's multifactorial nature is crucial for developing interventions. Targeting inflammation, proteolytic dysregulation, and metabolic issues may be effective. Anti-inflammatory therapies, protease inhibitors, and metabolic modulators could help preserve muscle mass and function, particularly in at-risk individuals.

4.2.2 Early Metabolic Destabilization in Presarcopenia

Presarcopenia refers to the early stages of sarcopenia, where muscle mass and function begin to decline but have not yet reached clinically significant levels [3]. Early metabolic destabilization in presarcopenia involves alterations in energy metabolism, insulin sensitivity, and mitochondrial function. These metabolic changes can precede

overt muscle loss and may contribute to the development of sarcopenia by impairing muscle energy production and utilization [42,43]. Understanding the mechanisms underlying early metabolic destabilization is crucial for developing interventions that can slow or prevent the progression of sarcopenia.

The clinical markers exhibited significant intergroup disparities in age, abdominal and hip circumferences, BMI, body fat percentage, ALM, ASMI, SPPB total score, and SarQoL domains. These findings underscore the multifaceted and complex nature of sarcopenia's impact on both physical performance and quality of life, highlighting the need for a comprehensive approach to its assessment and management.

To further elucidate the discriminatory power of these variables, a discriminant analysis was meticulously conducted to classify the groups. The results revealed a slight shift in the significance of the predictors. Specifically, the analysis identified waist-to-hip ratio (WHR), BMI, body fat content, lean mass, ASMI, SPPB score, physical activity levels (measured via the International Physical Activity Questionnaire — IPAQ), the physical health component of the SF-36, and certain SarQoL domains (D4, D5) as influential in distinguishing between the groups. These findings underscore the importance of a multifactorial approach in the diagnosis and classification of sarcopenia, emphasizing the integration of anthropometric, functional, and quality of life metrics to capture the full spectrum of the condition's impact.

4.2.3 Macrophages as Indicators of Muscle Tissue Status

Macrophages are immune cells that play a key role in tissue repair, regeneration, and inflammation. In the context of sarcopenia, macrophages can be indicators of muscle tissue status due to their involvement in muscle repair and inflammatory processes [6]. The balance between pro-inflammatory (M1) and anti-inflammatory (M2) macrophages is crucial for muscle homeostasis. An imbalance favoring M1 macrophages can promote inflammation and muscle damage, while M2 macrophages are involved in tissue repair and regeneration. Assessing the polarization and activity of macrophages in muscle tissue can provide valuable insights into the underlying mechanisms of sarcopenia and potential therapeutic targets [9,44]. For example, strategies aimed at modulating macrophage polarization towards an anti-inflammatory phenotype may help to reduce inflammation and support muscle repair in sarcopenia.

The distribution of CD14–CD163+206+ cells, exhibited significant disparities, underscoring the chronic inflammatory milieu associated with sarcopenia. The multivariate analysis further delineated immunological markers not discerned by the Kruskal–Wallis test, including CD14+CD163+ and CD14–CD163+ subpopulations, as well as CD68–CD163+ and CD68+CD163–206+ subsets.

These findings provide a nuanced understanding of the immunological landscape in sarcopenia, shedding light on potential therapeutic targets and mechanisms underlying this geriatric syndrome.

4.2.4 EVs as Integrative Markers of Sarcopenia

EVs are membrane-bound particles released by cells into the extracellular environment. They play a crucial role in cell-to-cell communication and can carry various bioactive molecules, including proteins, lipids, and nucleic acids [44–47]. In the context of sarcopenia, EVs can serve as integrative markers due to their ability to reflect the physiological and pathological status of muscle tissue. For example, changes in the composition and function of EVs released by muscle cells can indicate alterations in muscle metabolism, inflammation, and ECM remodeling [19,48]. Furthermore, EVs can influence the behavior of recipient cells, such as macrophages and fibroblasts, thereby modulating muscle repair and regeneration processes. Investigating the role of EVs in sarcopenia may provide new insights into the pathogenesis of the disease and identify potential biomarkers for early detection and monitoring of sarcopenia [49].

Vesicular markers, such as TIMP-1, are molecules that can be found in vesicles — small membrane structures released by cells. They play a crucial role in intercellular communication and can transport various biological molecules, including proteins, lipids, and nucleic acids. The significance of vesicular markers as integrative indicators lies in their ability to reflect the condition of both tissues and blood. This makes them valuable tools for diagnosing and monitoring various diseases [50,51].

TIMP-1 is one such vesicular marker that can be used to assess the state of tissues and blood. It is involved in regulating tissue remodeling, inflammation, and angiogenesis. The level of TIMP-1 in vesicles can change in various pathological conditions, such as cancer, cardiovascular diseases, fibrosis, and others.

As integrative indicators, vesicular markers, including TIMP-1, can provide information about the state of tissues and blood simultaneously. For example, changes in TIMP-1 levels in vesicles may indicate disturbances in tissue remodeling or inflammation processes, which may be associated with the development of certain diseases. Additionally, the analysis of vesicular markers can help in assessing the effectiveness of treatment and monitoring the patient's condition. Therefore, vesicular markers, such as TIMP-1, are valuable tools for investigating the state of tissues and blood, as well as for diagnosing and monitoring various diseases.

5. Conclusion

Sarcopenia, an aging-related condition marked by muscle mass, strength, and function decline, is intricately tied to the aging process. Recent research has uncovered

the key roles of chronic inflammation, proteolytic imbalance, and metabolic disturbances in its pathophysiology.

Muscle tissue undergoes changes in the CD14⁺CD163⁺206⁺ cell population, indicating a chronic inflammatory environment. These cells release pro-inflammatory cytokines that contribute to muscle degradation. Proteolytic dysregulation, characterized by an imbalance between elastase-like, trypsin-like and their inhibitors, such as α 1-antitrypsin, further accelerates muscle loss.

Chronic inflammation sets off proteolytic cascades that break down muscle proteins. Metabolic disorders impair energy production and nutrient use, perpetuating muscle wasting. This complex interplay underscores the need for a holistic approach to understanding sarcopenia's pathogenesis.

Biochemical markers play a crucial role in revealing the multifaceted nature of sarcopenia. Advanced analytical techniques, such as discriminant analysis, allow for the classification of individuals based on anthropometric (waist-to-hip ratio, BMI, lean mass), functional (appendicular skeletal muscle index), physical activity (IPAQ), and quality of life measures. This comprehensive approach helps identify high-risk individuals and deepens our understanding of sarcopenia's mechanisms.

Vesicular indicators, like TIMP-1, provide insights into tissue remodeling and inflammation. Encapsulated within extracellular vesicles, TIMP-1 regulates extracellular matrix homeostasis, angiogenesis, and inflammation, making it a vital biomarker. Changes in TIMP-1 levels reflect disturbances in tissue remodeling, offering valuable clues about muscle loss mechanisms.

Studying sarcopenia poses significant challenges due to external factors and individual variability, which complicate biomarker interpretation. Standardized assessment methods and integrating biochemical data with clinical parameters are essential for improving diagnostic accuracy and intervention efficacy. Future research should focus on developing new biomarkers and refining existing ones to enhance specificity and sensitivity, informing targeted therapies and improving quality of life.

Investigating biochemical markers in sarcopenia offers critical insights into its pathophysiology and progression. Examining markers related to inflammation, metabolism, mitochondrial function, extracellular matrix remodeling, and extracellular vesicles deepens our understanding of muscle loss and dysfunction. Addressing assessment and interpretation challenges will lead to more effective diagnostic and therapeutic strategies for this debilitating geriatric syndrome.

Availability of Data and Materials

The datasets used or analyzed during the current study are available from the corresponding author on reasonable request.

Author Contributions

Conceptualization, LVS and LMS; methodology, NVT; formal analysis, DAS and OEA; investigation, AIR, MPS and SMM; data curation, MVM, IGS, and IJO; validation, VAS and SST; draft the paper, DAS. All authors contributed to editorial changes in the manuscript. All authors read and approved the final manuscript. All authors have participated sufficiently in the work and agreed to be accountable for all aspects of the work.

Ethics Approval and Consent to Participate

The study was conducted in accordance with the Declaration of Helsinki, and approved by the Ethics Committee of the Siberian State Medical University (protocol No. 10000, dated January 20, 2024). Informed consent was obtained from all subjects involved in the study.

Acknowledgment

Not applicable.

Funding

This research received no external funding.

Conflict of Interest

Given her role as the Guest Editor, Liudmila V. Spirina had no involvement in the peer-review of this article and has no access to information regarding its peer review. Full responsibility for the editorial process for this article was delegated to Wei-Lin Jin and Amedeo Amedei.

Supplementary Material

Supplementary material associated with this article can be found, in the online version, at <https://doi.org/10.31083/FBL42063>.

References

- [1] Malmstrom TK, Morley JE. SARC-F: a simple questionnaire to rapidly diagnose sarcopenia. *Journal of the American Medical Directors Association*. 2013; 14: 531–532. <https://doi.org/10.1016/j.jamda.2013.05.018>.
- [2] Sattler MC, Jaunig J, Tösch C, Watson ED, Mokkink LB, Dietz P, *et al.* Current Evidence of Measurement Properties of Physical Activity Questionnaires for Older Adults: An Updated Systematic Review. *Sports Medicine (Auckland, N.Z.)*. 2020; 50: 1271–1315. <https://doi.org/10.1007/s40279-020-01268-x>.
- [3] Cruz-Jentoft AJ, Bahat G, Bauer J, Boirie Y, Bruyère O, Cederholm T, *et al.* Sarcopenia: revised European consensus on definition and diagnosis. *Age and Ageing*. 2019; 48: 16–31. <https://doi.org/10.1093/ageing/afy169>.
- [4] Altaf S, Malmir K, Mir SM, Olyaei GR, Aftab A, Rajput TA. Prevalence and associated risk factors of sarcopenia in community-dwelling older adults in Pakistan: a cross-sectional study. *BMC Geriatrics*. 2024; 24: 497. <https://doi.org/10.1186/s12877-024-05111-0>.
- [5] Yuan S, Larsson SC. Epidemiology of sarcopenia: Prevalence, risk factors, and consequences. *Metabolism: Clinical and Exper-*

- imental. 2023; 144: 155533. <https://doi.org/10.1016/j.metabol.2023.155533>.
- [6] Hernandez-Torres F, Matias-Valiente L, Alzas-Gomez V, Aranega AE. Macrophages in the Context of Muscle Regeneration and Duchenne Muscular Dystrophy. *International Journal of Molecular Sciences*. 2024; 25: 10393. <https://doi.org/10.3390/ijms251910393>.
- [7] Chen C, Peng H, Zeng Y, Dong G. CD14, CD163, and CCR1 are involved in heart and blood communication in ischemic cardiac diseases. *The Journal of International Medical Research*. 2020; 48: 300060520951649. <https://doi.org/10.1177/0300060520951649>.
- [8] Mota CMD, Madden CJ. Neural control of the spleen as an effector of immune responses to inflammation: mechanisms and treatments. *American Journal of Physiology. Regulatory, Integrative and Comparative Physiology*. 2022; 323: R375–R384. <https://doi.org/10.1152/ajpregu.00151.2022>.
- [9] Dalle S, Rossmeislova L, Kopko K. The Role of Inflammation in Age-Related Sarcopenia. *Frontiers in Physiology*. 2017; 8: 1045. <https://doi.org/10.3389/fphys.2017.01045>.
- [10] Yuan J, Zhang J, Luo Q, Peng L. Effects of nonalcoholic fatty liver disease on sarcopenia: evidence from genetic methods. *Scientific Reports*. 2024; 14: 2709. <https://doi.org/10.1038/s41598-024-53112-1>.
- [11] Tarantino G, Citro V, Balsano C. Liver-spleen axis in non-alcoholic fatty liver disease. *Expert Review of Gastroenterology & Hepatology*. 2021; 15: 759–769. <https://doi.org/10.1080/17474124.2021.1914587>.
- [12] Shiba N, Miyazaki D, Yoshizawa T, Fukushima K, Shiba Y, Inaba Y, *et al.* Differential roles of MMP-9 in early and late stages of dystrophic muscles in a mouse model of Duchenne muscular dystrophy. *Biochimica et Biophysica Acta*. 2015; 1852: 2170–2182. <https://doi.org/10.1016/j.bbdis.2015.07.008>.
- [13] Chen X, Li Y. Role of matrix metalloproteinases in skeletal muscle: migration, differentiation, regeneration and fibrosis. *Cell Adhesion & Migration*. 2009; 3: 337–341. <https://doi.org/10.4161/cam.3.4.9338>.
- [14] Araújo RF, Jr, Lira GA, Vilaça JA, Guedes HG, Leitão MCA, Lucena HF, *et al.* Prognostic and diagnostic implications of MMP-2, MMP-9, and VEGF- α expressions in colorectal cancer. *Pathology, Research and Practice*. 2015; 211: 71–77. <https://doi.org/10.1016/j.prp.2014.09.007>.
- [15] Buttacavoli M, Di Cara G, Roz E, Pucci-Minafra I, Feo S, Cancemi P. Integrated Multi-Omics Investigations of Metalloproteinases in Colon Cancer: Focus on MMP2 and MMP9. *International Journal of Molecular Sciences*. 2021; 22: 12389. <https://doi.org/10.3390/ijms222212389>.
- [16] Hadler-Olsen E, Solli AI, Hafstad A, Winberg JO, Uhlin-Hansen L. Intracellular MMP-2 activity in skeletal muscle is associated with type II fibers. *Journal of Cellular Physiology*. 2015; 230: 160–169. <https://doi.org/10.1002/jcp.24694>.
- [17] Jabłońska-Trypuć A, Matejczyk M, Rosochacki S. Matrix metalloproteinases (MMPs), the main extracellular matrix (ECM) enzymes in collagen degradation, as a target for anticancer drugs. *Journal of Enzyme Inhibition and Medicinal Chemistry*. 2016; 31: 177–183. <https://doi.org/10.3109/14756366.2016.1161620>.
- [18] Shimoda M. Extracellular vesicle-associated MMPs: A modulator of the tissue microenvironment. *Advances in Clinical Chemistry*. 2019; 88: 35–66. <https://doi.org/10.1016/bs.acc.2018.10.006>.
- [19] Ayloo S, Lazo CG, Sun S, Zhang W, Cui B, Gu C. Pericyte-to-endothelial cell signaling via vitronectin-integrin regulates blood-CNS barrier. *Neuron*. 2022; 110: 1641–1655.e6. <https://doi.org/10.1016/j.neuron.2022.02.017>.
- [20] Li H, Mittal A, Makonchuk DY, Bhatnagar S, Kumar A. Matrix metalloproteinase-9 inhibition ameliorates pathogenesis and improves skeletal muscle regeneration in muscular dystrophy. *Human Molecular Genetics*. 2009; 18: 2584–2598. <https://doi.org/10.1093/hmg/ddp191>.
- [21] Zhang Y, Yang P, Zhang X, Liu S, Lou K. Asprosin: its function as a novel endocrine factor in metabolic-related diseases. *Journal of Endocrinological Investigation*. 2024; 47: 1839–1850. <https://doi.org/10.1007/s40618-024-02360-z>.
- [22] Zhao Y, Wang Z, Chen Y, Feng M, Liu X, Chen H, *et al.* Asprosin aggravates atherosclerosis via regulating the phenotype transformation of vascular smooth muscle cells. *International Journal of Biological Macromolecules*. 2024; 268: 131868. <https://doi.org/10.1016/j.ijbiomac.2024.131868>.
- [23] Wang ZY, Li YM, Yan JJ, Wang Q, Zhao C, Lu X, *et al.* Low serum Metrn levels are associated with increased risk of sarcopenia in the older adults. *European Geriatric Medicine*. 2024; 15: 1849–1857. <https://doi.org/10.1007/s41999-024-01074-y>.
- [24] Daily JW, Park S. Sarcopenia Is a Cause and Consequence of Metabolic Dysregulation in Aging Humans: Effects of Gut Dysbiosis, Glucose Dysregulation, Diet and Lifestyle. *Cells*. 2022; 11: 338. <https://doi.org/10.3390/cells11030338>.
- [25] Massimino E, Izzo A, Riccardi G, Della Pepa G. The Impact of Glucose-Lowering Drugs on Sarcopenia in Type 2 Diabetes: Current Evidence and Underlying Mechanisms. *Cells*. 2021; 10: 1958. <https://doi.org/10.3390/cells10081958>.
- [26] Al Saedi A, Debruin DA, Hayes A, Hamrick M. Lipid metabolism in sarcopenia. *Bone*. 2022; 164: 116539. <https://doi.org/10.1016/j.bone.2022.116539>.
- [27] Chen MJ, Leng J, Ni JP, Xiong AL, Hu MY. U-shaped association between plasma C-peptide and sarcopenia: A cross-sectional study of elderly Chinese patients with diabetes mellitus. *PloS One*. 2023; 18: e0292654. <https://doi.org/10.1371/journal.pone.0292654>.
- [28] Jalal M, Rosendahl J, Campbell JA, Vinayagam R, Al-Mukhtar A, Hopper AD. Identification of “Digital Sarcopenia” Can Aid the Detection of Pancreatic Exocrine Insufficiency and Malnutrition Assessment in Patients with Suspected Pancreatic Pathology. *Digestive Diseases (Basel, Switzerland)*. 2022; 40: 335–344. <https://doi.org/10.1159/000517554>.
- [29] Matsumura D, Kawao N, Okumoto K, Ohira T, Mizukami Y, Akagi M, *et al.* Effects of elastase-induced emphysema on muscle and bone in mice. *PloS One*. 2023; 18: e0287541. <https://doi.org/10.1371/journal.pone.0287541>.
- [30] Han M, Woo K, Kim K. Association of Protein Intake with Sarcopenia and Related Indicators Among Korean Older Adults: A Systematic Review and Meta-Analysis. *Nutrients*. 2024; 16: 4350. <https://doi.org/10.3390/nu16244350>.
- [31] Li SY, Lu ZH, Leung JCS, Kwok TCY. Association of dietary protein intake, inflammation with muscle mass, physical performance and incident sarcopenia in Chinese community-dwelling older adults. *The Journal of Nutrition, Health & Aging*. 2024; 28: 100163. <https://doi.org/10.1016/j.jnha.2024.100163>.
- [32] Jarosch I, Gehlert S, Jacko D, Koczulla RA, Wencker M, Welte T, *et al.* Different Training-Induced Skeletal Muscle Adaptations in COPD Patients with and without Alpha-1 Antitrypsin Deficiency. *Respiration; International Review of Thoracic Diseases*. 2016; 92: 339–347. <https://doi.org/10.1159/000449509>.
- [33] Théry C, Witwer KW, Aikawa E, Alcaraz MJ, Anderson JD, Andriantsitohaina R, *et al.* Minimal information for studies of extracellular vesicles 2018 (MISEV2018): a position statement of the International Society for Extracellular Vesicles and update of the MISEV2014 guidelines. *Journal of Extracellular Vesicles*. 2018; 7: 1535750. <https://doi.org/10.1080/20013078.2018.1535750>.
- [34] Holden JE, Finch WH, Kelley K. A Comparison of Two-Group Classification Methods. *Educational and Psychological Measurement*. 2011; 71: 870–901. <https://doi.org/10.1177/0013164411398357>.

- [35] Huberty CJ, Olejnik S. Applied MANOVA and Discriminant Analysis. 1st edn. Wiley: Hoboken, New Jersey, USA. 2006.
- [36] McLachlan GJ. Discriminant Analysis and Statistical Pattern Recognition. 1st edn. Wiley: New York, USA. 1992.
- [37] Lever J, Krzywinski M, Altman N. Principal component analysis. *Nature Methods*. 2017; 14: 641–642. <https://doi.org/10.1038/nmeth.4346>.
- [38] Welsh JA, Goberdhan DCI, O'Driscoll L, Buzas EI, Blenkiron C, Bussolati B, *et al.* Minimal information for studies of extracellular vesicles (MISEV2023): From basic to advanced approaches. *Journal of Extracellular Vesicles*. 2024; 13: e12404. <https://doi.org/10.1002/jev2.12404>.
- [39] Alameddine HS. Matrix metalloproteinases in skeletal muscles: friends or foes? *Neurobiology of Disease*. 2012; 48: 508–518. <https://doi.org/10.1016/j.nbd.2012.07.023>.
- [40] Zhou P, Yang C, Zhang S, Ke ZX, Chen DX, Li YQ, *et al.* The Imbalance of MMP-2/TIMP-2 and MMP-9/TIMP-1 Contributes to Collagen Deposition Disorder in Diabetic Non-Injured Skin. *Frontiers in Endocrinology*. 2021; 12: 734485. <https://doi.org/10.3389/fendo.2021.734485>.
- [41] Spitzberg JD, Ferguson S, Yang KS, Peterson HM, Carlson JCT, Weissleder R. Multiplexed analysis of EV reveals specific biomarker composition with diagnostic impact. *Nature Communications*. 2023; 14: 1239. <https://doi.org/10.1038/s41467-023-36932-z>.
- [42] Pradhan BS, Prószyński TJ. A Role for Caveolin-3 in the Pathogenesis of Muscular Dystrophies. *International Journal of Molecular Sciences*. 2020; 21: 8736. <https://doi.org/10.3390/ijms21228736>.
- [43] Hoh JFY. Developmental, physiologic and phylogenetic perspectives on the expression and regulation of myosin heavy chains in mammalian skeletal muscles. *Journal of Comparative Physiology. B, Biochemical, Systemic, and Environmental Physiology*. 2023; 193: 355–382. <https://doi.org/10.1007/s00360-023-01499-0>.
- [44] Agnetti G, Herrmann H, Cohen S. New roles for desmin in the maintenance of muscle homeostasis. *The FEBS Journal*. 2022; 289: 2755–2770. <https://doi.org/10.1111/febs.15864>.
- [45] Linke WA. Stretching the story of titin and muscle function. *Journal of Biomechanics*. 2023; 152: 111553. <https://doi.org/10.1016/j.jbiomech.2023.111553>.
- [46] Shoemaker ME, Pereira SL, Mustad VA, Gillen ZM, McKay BD, Lopez-Pedrosa JM, *et al.* Differences in muscle energy metabolism and metabolic flexibility between sarcopenic and nonsarcopenic older adults. *Journal of Cachexia, Sarcopenia and Muscle*. 2022; 13: 1224–1237. <https://doi.org/10.1002/jcsm.12932>.
- [47] Affourtit C, Carré JE. Mitochondrial involvement in sarcopenia. *Acta Physiologica (Oxford, England)*. 2024; 240: e14107. <https://doi.org/10.1111/apha.14107>.
- [48] Kraakman MJ, Murphy AJ, Jandeleit-Dahm K, Kammoun HL. Macrophage polarization in obesity and type 2 diabetes: weighing down our understanding of macrophage function? *Frontiers in Immunology*. 2014; 5: 470. <https://doi.org/10.3389/fimmu.2014.00470>.
- [49] Becker A, Thakur BK, Weiss JM, Kim HS, Peinado H, Lyden D. Extracellular Vesicles in Cancer: Cell-to-Cell Mediators of Metastasis. *Cancer Cell*. 2016; 30: 836–848. <https://doi.org/10.1016/j.ccell.2016.10.009>.
- [50] Liu Z, Liu Y, Li Y, Xu S, Wang Y, Zhu Y, *et al.* ECM stiffness affects cargo sorting into MSC-EVs to regulate their secretion and uptake behaviors. *Journal of Nanobiotechnology*. 2024; 22: 124. <https://doi.org/10.1186/s12951-024-02411-w>.
- [51] Li C, Wu Q, Li Z, Wang Z, Tu Y, Chen C, *et al.* Exosomal microRNAs in cancer-related sarcopenia: Tumor-derived exosomal microRNAs in muscle atrophy. *Experimental Biology and Medicine (Maywood, N.J.)*. 2021; 246: 1156–1166. <https://doi.org/10.1177/1535370221990322>.